

A Bipolar Repeater for Pulse Code Modulation Signals

By J. S. MAYO

(Manuscript received July 12, 1961)

Designed for use on unloaded exchange cable, this repeater was developed to satisfy the transmission requirements of an experimental PCM system. It utilizes a pulse repetition frequency of 1.544 mc, and 6000-ft repeater spacing. Functionally, the repeated line transmits the PCM signal without appreciable degradation over distances up to 25 miles, a feat accomplished by retiming and reshaping the signal at each repeater point. Retiming is accomplished by means of a clock extracted from the signal; reshaping is accomplished by regeneration with positive pulse width control.

Near-end crosstalk and pulse train jitter dominate the design parameters. Timing is made tolerant of near-end crosstalk by choice of bipolar transmission (where successive marks are of opposite polarity) with clock derived from the rectified and clipped signal. Tolerance in the decision circuit is obtained by automatic threshold control, spike sampling, and tight control of time and voltage parameters. Accumulated pulse train jitter is controlled to the extent dictated by the terminal equipment, principally through control of the bandwidth of the clock circuit.

Seven diffused-base transistors and ten logic diodes are used in the one-way repeater circuit. A two-way repeater consists of two such circuits with a common power unit, utilizes 135 components, and is packaged in a can of $1\frac{1}{6} \times 3\frac{1}{8} \times 5\frac{3}{4}$ -inches outside dimensions. Accommodations are made for line-length and power options, as well as remote testing. Power for the repeater is transmitted over the signal pair. One watt is required for the two-way repeater.

I. INTRODUCTION

Companion papers^{1,3,6} propose transmission of 24 voice channels by means of pulse code modulation over 22-gauge paper insulated cable pairs. Seven-digit coding, built-in signaling, and frame synchronization dictate a 1.544-mc pulse rate. Very simply, the repeater function is to

"look" at a received pulse train and emit a "new" pulse for each received pulse, a feat that becomes impossible when the transmission bandwidth is sufficiently limited, or the noise environment is sufficiently strong that realizable circuitry cannot distinguish pulse from interference. In practice these parameters are controlled by repeater spacing, and installation of repeaters is greatly inconvenienced if the nominal spacing is 6000 feet (a repeater then replaces a load coil). Such spacing produces a very difficult interference situation.

One of the many virtues of PCM is that the pulse train carries its own timing information, and this paper considers only the self-timed repeater. In such repeaters it is essential that the recovered clock be and remain phase locked to the incoming pulse train, even in the presence of severe interference.

Interference is mainly intra- or inter-system crosstalk via the near-end crosstalk path (NEXT). Such interference is strongest at high frequencies where timing information must be transmitted. A second important interference source is office impulse noise, which is confined to the vicinity of offices and requires shortened repeater spacing adjacent to offices. Interference of PCM into other carrier systems and vice-versa is considered briefly by Aaron.¹

Manhole mounting of repeaters is anticipated and repeater size is of utmost importance. Extreme reliability is required, and excessive component miniaturization may not only jeopardize reliability but be costly besides. A reasonable compromise is the use of standard, well-known components with diminutive repeater size achieved by high packing density.

The repeater must withstand environmental conditions attendant to field mounted equipment, including lightning surge activity. A repeater should require no adjustments other than those made at time of manufacture.

Operating error rate per system should be of the order of one error in the most significant digit per channel per minute. This produces one audible click per channel per minute and corresponds to a pulse error rate of the order of one error per 10^6 time slots.

II. FEATURES

The following items summarize the design considerations.

2.1 *Bipolar Transmission*

At the pulse repetition rate, about one per cent of the NEXT paths have less loss than maximum line loss. Transmission of clock at this

rate leads to a very difficult near-end crosstalk situation. A solution is to transmit the clock at less than the bit rate. Aaron¹ presents the problem, considers many transmission schemes, and chooses 50 per cent duty-cycle bipolar transmission where successive marks are of opposite polarity because: (1) by obtaining a 1.5-mc clock from rectification of the bipolar train, most of the clock energy comes from midband (750 ke) where line loss is about 15 db less than at the bit rate, (2) by transmitting clock at half the bit rate, half bit-rate crosstalk loss is applicable, (3) by clipping the pulse train before clock extraction, baseline noise is removed, easing the adverse pulse density problem of sparse transmitted pattern-dense interfering pattern, and (4) by utilizing a transmission scheme with concentration of energy at midband, spectral nulls at zero frequency and the bit rate, physical realization is not so difficult.

2.2 Threshold and Clipping Control

Of the many methods of pulse recognition, comparison of the received pulse amplitude to a reference is by far the easiest to implement. With a fixed reference of half the nominal pulse height, a theoretical limit of 6-db reduction in received pulse height exists. A smaller reference accommodates a smaller pulse but also accommodates less noise, and indeed may be exceeded by the tail of a large pulse. Because (1) the received signal is subject to 6- to 12-db amplitude variations from location to location in the environment considered, (2) a pulse will interfere into an adjacent time slot, (3) field gain adjustments are undesirable, and (4) good noise performance is a decided goal, it is essential that the reference "threshold" be dependent upon the average received pulse amplitude. Also the clipping level in the clock path must be proportional to received signal amplitude. Otherwise the phase of the recovered clock would be dependent upon the amplitude of the received signal. It conveniently results that the same signal-dependent voltage (equal to approximately half the peak received signal) may be used in both the "threshold" and clock circuits.

2.3 Spike Sampling

The recovered clock zero-crossings tell where to "look" on the pulse train. To prevent partial pulsing, to optimize crosstalk performance, and to allow maximum phase instability in the recovered clock circuit, a narrow sampling pulse must be used to examine the received pulse train.

2.4 *Width Control*

Optimum line equalization results in rise-time limited transmission, the received pulse amplitude being proportional to both the height and width of the transmitted pulse. Good performance requires control of transmitted pulse width, particularly to make it independent of pattern or random variations. The use of the recovered clock for this purpose is most attractive, the positive-going clock zero-crossing "starts" the output pulse, the negative-going zero-crossing "stops" it.

2.5 *Powering*

Powering of repeaters over the cable pair is most attractive. For the exchange plant, interoffice distances up to 25 miles must be spanned. Half that distance must be powerable from each office, preferably with existing power supplies. Because of line resistance, maximum power available per two-way repeater is approximately one watt, and this requires both $+130$ and -130 volts at each end of the 25-mile system.

III. CONFIGURATION

The stage has been set for the configuration of Fig. 1. The received pulse train is acted upon by linear shaped gain to produce an optimum signal-to-noise condition at the output. The preamplifier gain characteristic is set by the characteristic of 6000 feet of cable. Lesser cable lengths are accommodated by selected quantized line-build-out (LBO) networks that make any cable length appear as approximately 6000 feet to the preamplifier. An average preamplifier output level is established by the automatic threshold and clipping circuit. Rectified and clipped pulses enter a tuned circuit of high Q to produce a sine-wave clock. The zero crossings of the sine wave are extracted and delivered to the regenerator as "sample" and "turn-off" pulses. The regenerator puts out a "new" pulse when the preamplifier output exceeds the reference during the sampling instant. For bipolar transmission the regenerator is a "balanced" circuit of identical halves in push-pull. Positive pulses are automatically routed through one half of the regenerator and negative pulses through the other half. The repeater is thus in a sense not a bipolar repeater, but a generalized pseudo-ternary repeater, theoretically capable of handling any 50 per cent duty cycle pseudo-ternary code that has no zero frequency component.

The arguments have led to a forward-acting repeater with complete retiming and pulse width control. Comparison with other repeater arrangements has been made by Aaron.¹

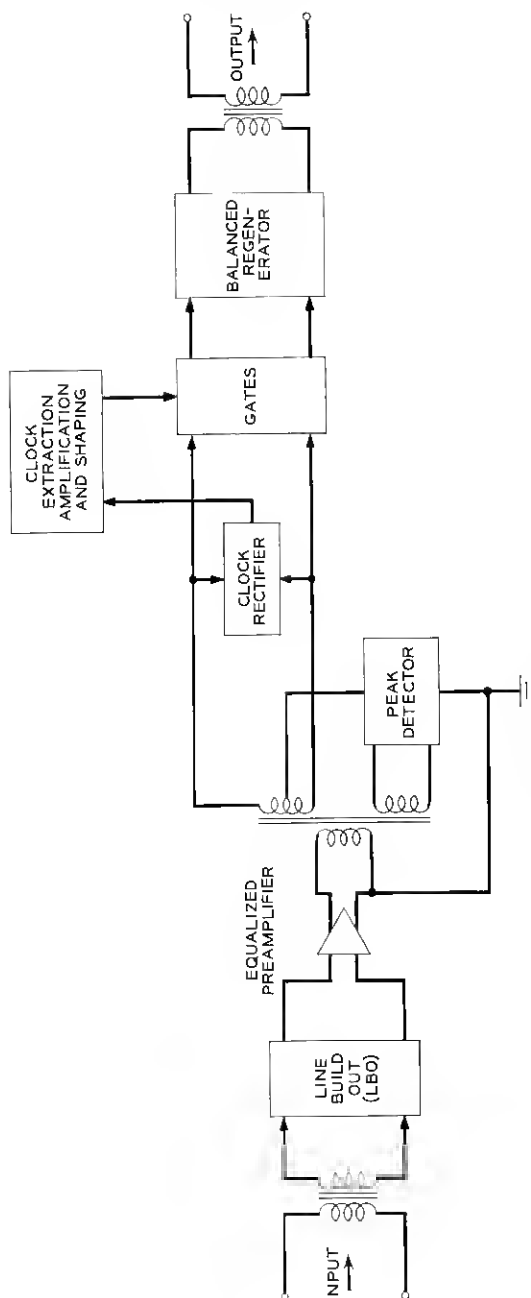


Fig. 1 — Repeater configuration.

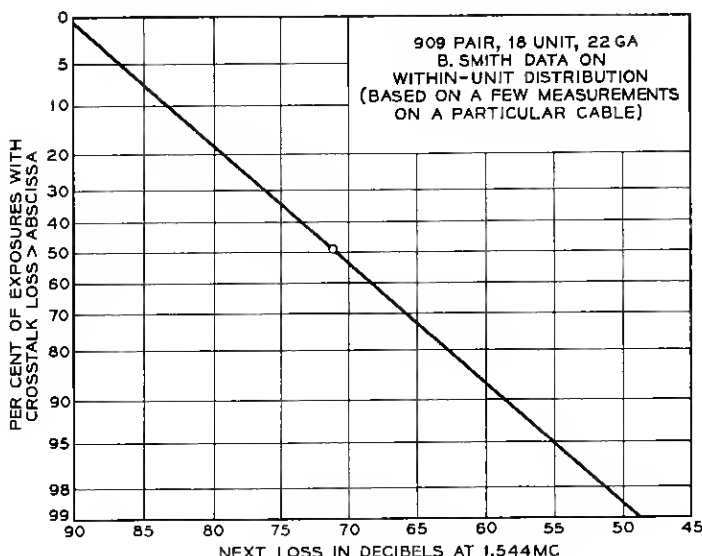


Fig. 2 — Distribution of near-end crosstalk loss.

IV. EQUALIZATION OPTIMIZATION

Define optimum equalization as that cable-LBO-preamplifier gain-frequency characteristic which allows maximum NEXT coupling for the condition of marginal pulse detection. This optimum will be dependent not only upon the cable and crosstalk path characteristics, but upon the "goodness" of the detection process — that is, how accurately the clock spike and threshold positions can be held. Good time cross-hair positioning with poor voltage crosshair control dictates a characteristic quite different from the optimum for good voltage but poor time control. Optimization on a crosstalk basis applies primarily to the case of nominal line lengths, where near-end crosstalk is important. Short line lengths are likely to be near offices where optimization on the basis of impulse noise immunity is important. A reasonable approach is to shape the preamplifier for good crosstalk performance for 6000 feet of cable, then design the LBO to optimize impulse noise performance.

Fig. 2 shows the distribution of near-end crosstalk loss for 22CSA cable.* The distribution appears to be log normal with about 1 per cent of the couplings having less than 49 db loss at 1.5 mc. The coupling loss decreases with frequency, in the band of interest, at a rate of ap-

* Aaron¹ considers the cable loss and crosstalk characteristics in some detail. The curve presented is based on a small number of samples on a particular cable.

proximately 4.5 db per octave. No truncation of the distribution is indicated in Fig. 2, though common sense would indicate some lower limit must exist.

Approximate 6000-ft cable response is shown in Fig. 3. Superimposing the 1 per cent crosstalk limit vividly shows that the usable transmission band does not quite extend up to the 1.5-mc bit rate.

A random 50 per cent duty-cycle bipolar pulse train $p(t)$ starting at $t = 0$ with the first pulse positive has a Laplace transform given by

$$P(s) = \frac{1}{s} \left[1 - \exp \frac{-sT_0}{2} \right] \sum_0^{\infty} a_n e^{-nsT_0} \quad (1)$$

where T_0 = pulse repetition period and

$$a_n = 1, 0, -1 \quad \text{under the bipolar constraint} \quad \sum_0^k a_n = 0, 1.$$

Transmission of this train over a cable and an equalized amplifier of over-all transfer function $G(s)$ gives a signal

$$R(s) = \frac{G(s)}{s} \left[1 - \exp \frac{-sT_0}{2} \right] \sum_0^{\infty} a_n e^{-nsT_0} = L \{ r(t) \}. \quad (2)$$

This signal must be compared to a reference voltage periodically to determine the presence or absence of a pulse.

Let $H(s)$ represent the over-all NEXT path and amplifier characteristic, so the crosstalk signal $N(s)$ at the decision point is

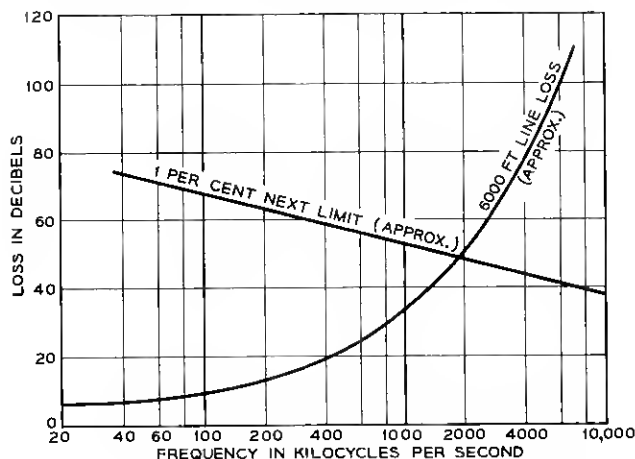


Fig. 3 — Line loss and NEXT loss as a function of frequency.

$$N(s) = \frac{H(s)}{s} \left[1 - \exp \frac{-sT_1}{2} \right] \sum_0^{\infty} b_n e^{-nsT_1} = L\{n(t)\} \quad (3)$$

where b_n describes the interfering pattern and $1/T_1$ the interfering frequency. With an amplifier characteristic $A(s)$ and a NEXT path described by ks (an approximation), and the cable characteristic by $C(s)$,

$$G(s) = C(s)A(s) \quad (4)$$

$$H(s) = ksA(s) \quad (5)$$

$$H(s) = ks \frac{G(s)}{C(s)} \quad (6)$$

$$N(s) = k \frac{G(s)}{C(s)} \left[1 - \exp \frac{-sT_1}{2} \right] \sum_0^{\infty} b_n e^{-nsT_1}. \quad (7)$$

A good approximation for the cable characteristic of Fig. 3 must consider a matching of time response. A fair approximation in the range of interest is

$$C(s) = \frac{0.4}{\left(\frac{s}{\omega_1} + 1\right) \left(\frac{s}{\omega_2} + 1\right)} \quad (8)$$

where $\omega_1 = 2\pi \times 80$ kc and $\omega_2 = 2\pi \times 800$ kc.

It is desired to solve (2), (7), and (8) for that $G(s)$ which maximizes k for a workable $r(t)/n(t)$ ratio at decision instants. With $r(t)$ and $n(t)$ asynchronous, for error rates of 1 in 10^6 , it is necessary to consider only $n(t)_{\max}$ which adds or subtracts from $r(t)$ to form the composite signal upon which decisions must be made. Furthermore, $H(s)$ has accentuated high-frequency response, so each crosstalk pulse is pretty well confined to its own time slot and $n(t)_{\max}$ may be computed from (7) with $b_0 = 1$ and $b_j = 0, j \geq 1$.

Such an assumption does not hold for the severely band-limited signal path. Generally, however, in a workable situation the received signal is confined to 3 time slots, a received pulse being principally affected only by the one preceding it and the one following it. From (2), $r(t)$ may be computed for three important cases:

$$\text{Case 1:} \quad a_{j-1} = 1, \quad a_k = 0, \quad k \neq j-1 \quad (9)$$

$$\text{Case 2:} \quad a_{j+1} = 1, \quad a_k = 0, \quad k \neq j+1 \quad (10)$$

$$\begin{aligned} \text{Case 3:} \quad a_{j-1} = -1, \quad a_j = 1, \quad a_{j+1} = -1, \\ a_k = 0, \quad k \neq j-1, j, j+1. \end{aligned} \quad (11)$$

Case 1 gives the interference of a pulse in $j - 1$ time slot into the j th time slot. Case 2 gives the interference of a pulse in the $j + 1$ time slot into the j th time slot. The bipolar rule does not allow Case 1 and Case 2 to apply simultaneously. With a pulse in the j th time slot, only Case 3 is of real interest, where interference of adjacent pulses is most severe. For various $G(s)$, both signal and interference may be computed. Typical solutions for the signal are given in Fig. 4.

The area of Fig. 4 above Case 1 and Case 2 enclosed by Case 3 is the working area for detection. In the absence of any interference, the voltage and time crosshairs must intersect within this area. This area is referred to as an (worst case) "eye," and a chart of all eyes as the "eye diagram," which is just an oscilloscopic type display of a random pulse train. A typical eye diagram is shown in Fig. 5. It is seen to be symmetrical due to bipolar transmission.

Fig. 6 shows eye parameters of interest: the height, h , of the maximum opening which occurs at time T_m and the breadth, w , which occurs at amplitude E_t (generally taken so as to divide h into two equal parts). Let one half the difference between the height of an isolated pulse, E_m , at time T_m , and h define I , intersymbol interference,

$$I = \frac{1}{2}[E_m - h]. \quad (12)$$

Peak crosstalk interference hinders pulse recognition when, as seen in Fig. 4, it adds to Case 1 and Case 2 and when it subtracts from Case 3.

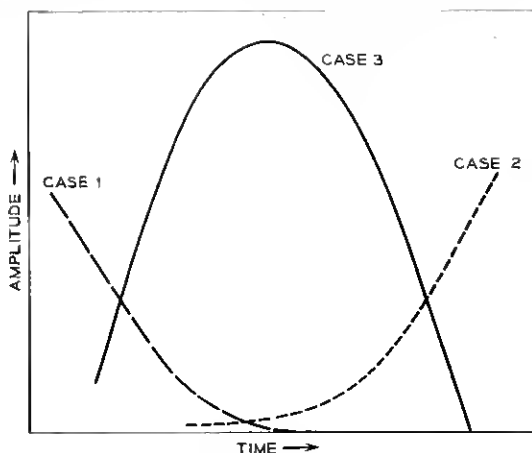


Fig. 4 — Typical received signal.

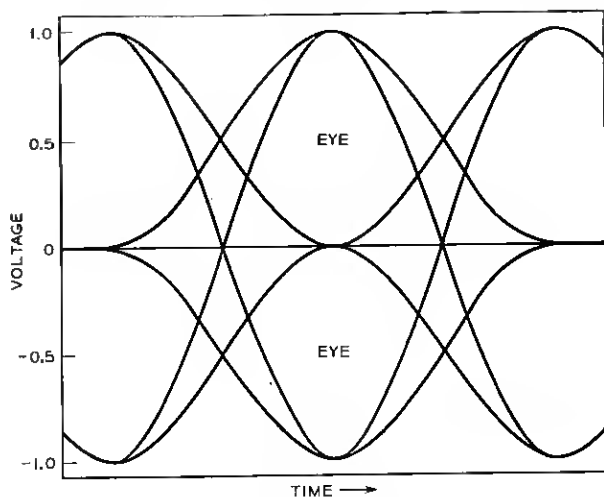


Fig. 5 — Eye diagram.

The maximum allowable interference is $h/2$, at which time the eye is closed.

Preliminaries aside, under the stated assumptions, for any $G(s)$ one may compute h and $n(t)_{\max}$. The value of k which makes $n(t)_{\max} = h/2$ defines the minimum crosstalk loss for which a repeater may work with a *single* interferer, and no other source of interference.

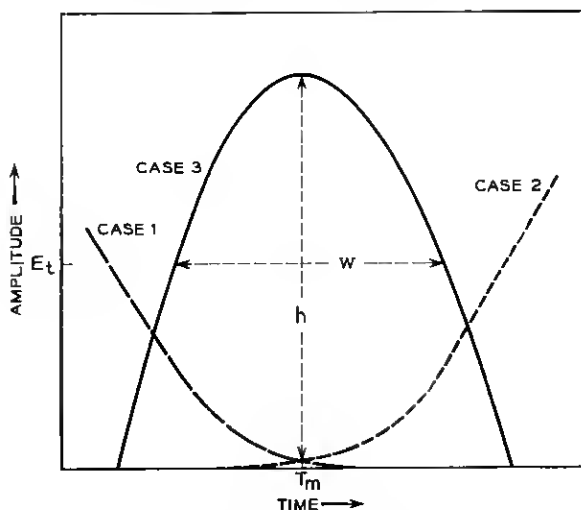


Fig. 6 — Eye parameters.

4.1 Gross Features

A convenient choice for $G(s)$ is*

$$G(s) = \frac{1}{\left(\frac{s}{2\pi f_i} + 1\right)^\alpha} \cdot \frac{s^2}{(s + \omega_3)(s + \omega_4)} \quad (13)$$

where f_i largely determines the bandwidth and α the rate of rolloff. ω_3 and ω_4 describe the low-frequency cutoffs that may be expected in the input and output transformers.

TABLE I — VALUE of $h(f_i, \alpha)$

$\frac{\alpha}{f_i}$	3	4	5
1.5 mc	0.90	0.90	0.95
1.25 mc	0.92	0.94	1.0
1.0 mc	0.98	0.93	0.78
0.75 mc	0.80	0.63	0.53

Solving (2) for Cases 1, 2 and 3, and computing h , one gets Table I, for transformer cutoffs at 20 and 40 kc, and henceforth taking $E_m = 1$. Equation (7) yields $n(t)_{\max}$, giving Table II.

TABLE II — VALUES OF $n(t)_{\max} \times 10^{-9} \times k^{-1}$

$\frac{\alpha}{f_i}$	3	4	5
1.5 mc	0.55	0.30	0.20
1.25 mc	0.43	0.22	0.14
1.0 mc	0.31	0.15	0.09
0.75 mc	0.19	0.07	0.05

The margin of operation in pulse detection, M , is

$$M = \frac{h}{2} - n(t)_{\max} \quad (14)$$

and by (12)

$$M = 0.5 - I - n(t)_{\max} \quad (15)$$

Near-end crosstalk loss at 1.544 mc is given by

$$x = -20 \log k - 140 \text{ db.} \quad (16)$$

* Aaron arrives at essentially the same result using the Gaussian cutoff. Equation (13) is not a bad representation of what one can do short of conditioning the equalization to the cable type, gauge or exact length.

Since

$$n(t)_{\max} = 10^9 qk \quad (17)$$

where q are the entries of Table II,

$$M = 0.5 - I - q[10^{(40-x)/20}]. \quad (18)$$

Equation (18) is plotted in Fig. 7 for various f_i and α .

A typical curve is shown in Fig. 8. As $x \rightarrow \infty$, $n(t) \rightarrow 0$; so the differ-

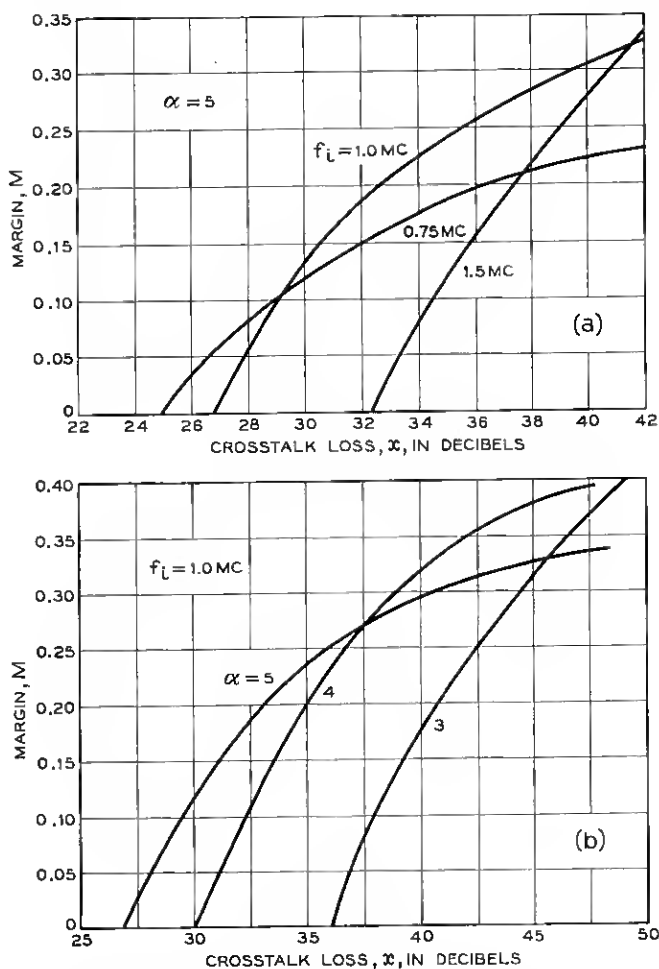


Fig. 7 — Margin as a function of x for (a) various f_i and (b) various α .

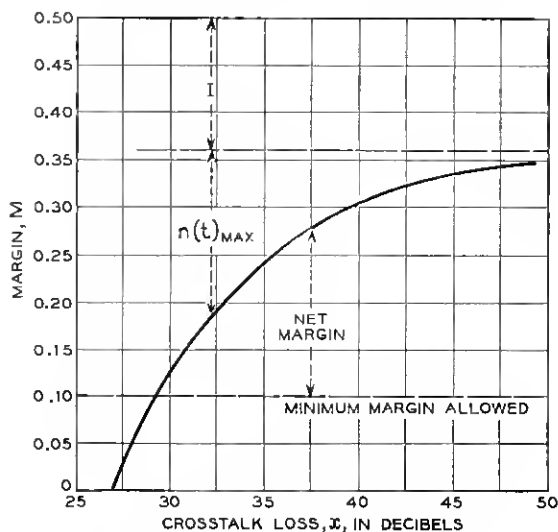


Fig. 8 — Typical margin-crosstalk curve.

ence between 0.5 and the asymptotic value of each curve of Fig. 7 gives intersymbol interference. For any x , the difference between the asymptotic value of each curve and the value of the curve gives the peak crosstalk signal. A narrow transmission band with sharp cutoff is indicated as optimum for the closed eye condition ($M = 0$). On the other hand, perfect threshold setting is unrealizable; the decision level is a region rather than a line; and some minimum M is required for a practical repeater. A reasonable figure is

$$M_{\min} = 0.1 \quad (19)$$

so the region below $M = 0.1$ on Fig. 7 is not usable. Very near optimum performance is obtained with a 1-mc cutoff and a 30 db per octave slope, giving,

$$G(jf) = \frac{1}{(1 + jf)^5}, \quad \text{with } f \text{ in mc and } f > 0.1. \quad (20)$$

Transmission through $G(jf)$ results in the pulse shape of Fig. 9. It is seen the pulse is not symmetrical, and some improvement should be obtainable via additional equalization.

4.2 Fine Features

Appropriately, one might now consider other forms for $G(jf)$ to achieve near optimum phase equalization. One may indeed proceed to choose a

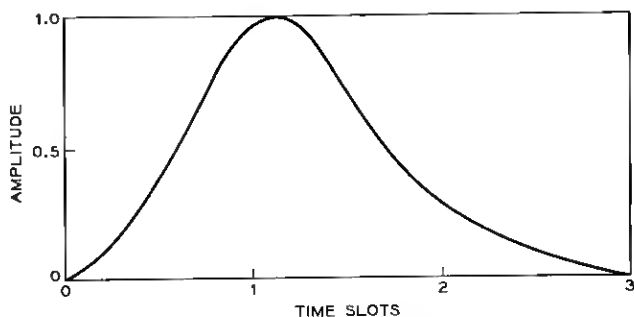


Fig. 9 — Pulse shape resulting from transmission through $G(jf)$.

function of known performance, such as one of the Thomson functions,¹⁰ and design an equalized amplifier-cable characteristic that closely approximates this function. Such was the course taken; but two difficulties arose. First, to achieve reasonably symmetrical pulses, higher-order Thomson functions are required. These lead to a very complicated equalizer (in terms of number of components). Secondly, statistical and length variation in the cable do not allow precise equalization short of a field equalizer adjustment, made for each repeater at time of installation.

Equalizer development, herein, follows a course of realization of a fairly simple characteristic of near optimum bandwidth and controlled cutoff, leading to a reasonable, but asymmetrical, time response. A nonlinear technique is then applied to reduce intersymbol interference in a manner not so critical of the exact cable characteristic.

4.2.1 Preamplifier Design

Several factors point to a feedback preamplifier with the cable equalizer characteristic built into the feedback path. Feedback is required to achieve gain stability. By placing the equalizer in the feedback loop, a large amount of feedback exists at lower frequencies, greatly reducing the output impedance — a very important consideration because the load driven by the preamplifier is decidedly nonlinear.

From a power gain point of view, a two-transistor amplifier is sufficient. The ac configuration chosen is shown in Fig. 10. The ac feedback network is shown in Fig. 11. Functionally, R_3 and C_2 allow the closed loop gain to rise at 6 db per octave, starting at 80 kc, to match the cable response falloff. At higher frequencies, the rising gain is checked and the rolloff established by R_1 , L_1 and Z_f .

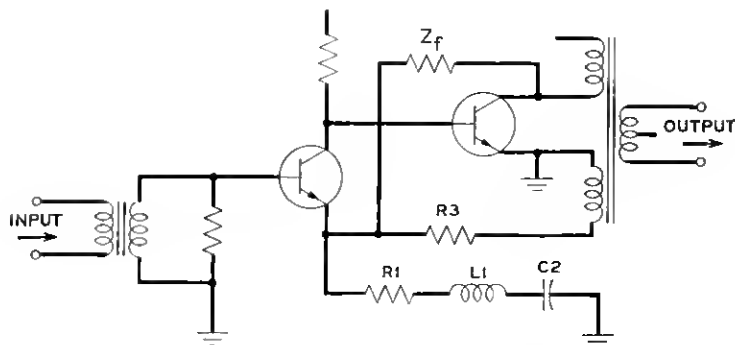


Fig. 10 — AC configuration of preamplifier.

From Fig. 11,

$$\frac{e_1}{e_0} = \frac{n}{1 + \frac{nR_3}{Z_f}} \left[1 + \frac{R_3}{Z_e} + \frac{R_3}{Z_f} \right] \quad (21)$$

which for large amounts of feedback is the closed-loop gain of the amplifier, K_v ,

$$K_v = \frac{n}{Z_f + nR_3} \frac{Z_e Z_f + R_3 Z_f + R_3 Z_e}{Z_e}. \quad (22)$$

Or

$$K_v = 1 + \frac{\frac{Z_f(nR_3)}{Z_f + nR_3}}{\frac{Z_e \left(\frac{nR_3}{n-1} \right)}{Z_e + \frac{nR_3}{n-1}}} \quad (23)$$

and if $Z_F(s)$ is the parallel combination of Z_f and nR_3 , and $Z_R(s)$ is the

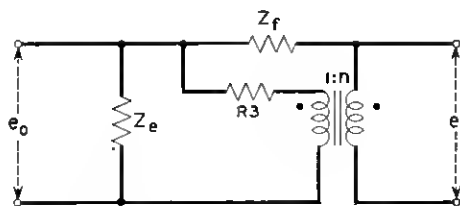


Fig. 11 — Feedback network configuration.

parallel combination of Z_e and $nR_3/(n-1)$,

$$K_v = 1 + \frac{Z_F(s)}{Z_E(s)}. \quad (24)$$

Neglecting the effects of transistor and transformer cutoffs, the voltage gain may be shaped according to (24) by proper selection of R_3 , Z_e and Z_f . Z_e has been chosen as a simple series RLC circuit, and Z_f has been chosen as the parallel combination of two RLC circuits, both as shown in Fig. 12.

The parameter n is chosen to give the desired low-frequency gain. Considering the low-frequency cable loss, the voltage gain of the input transformer, and the loss of amplitude due to the bandlimited transmission, one readily establishes $n = 3$ if peak preamplifier output is to equal the transmitted pulse height (3 volts). The combination R_3 , C_2 is chosen to give a zero of K_v (24) to cancel the effects of the 80-kc pole in the cable characteristic $C(s)$ (8). The rising gain is checked at 800 kc by C_3 , and the rolloff is started by the pole of $C(s)$. The preamplifier gain starts to fall at 1.5 mc due to L_1 and has a decided null (for repeater timing considerations) at 2.25 mc due to L_3 and C_4 . The response above 2.25 mc is suppressed by the L_2R_2 combination.

For the parameter values of Fig. 12, one may evaluate $Z_F(s)$ and $Z_E(s)$.

$$Z_E(s) = 0.705 \frac{s^2 + 0.9091s + 0.9183}{s^2 + 22.27s + 0.9183} \quad (25)$$

$$Z_F(s) = 0.5198 \frac{(s^2 + 0.1s + 1.961)(s^2 + 1.2195s + 4.545)}{s^4 + 3.429s^3 + 4.5396s^2 + 8.0376s + 3.2627} \quad (26)$$

where Z is in kilohms and s in units of 10^7 radians per second.

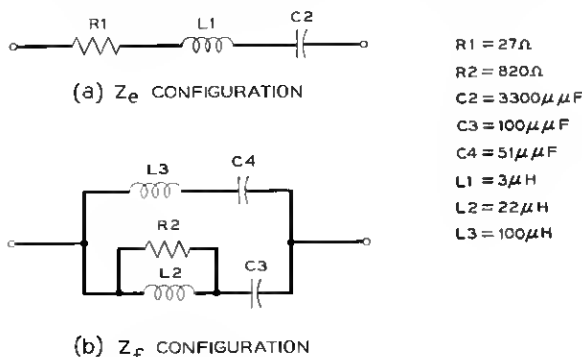


Fig. 12 — Network configurations; (a) Z_e configuration; (b) Z_f configuration.

By (24), the poles and zeros of K_v in megacycles per second are

<i>Poles</i>	<i>Zeros</i>
-0.800	-0.0928
-0.724 ± $j1.342$	-0.0965 ± $j2.22$
-0.193 ± $j2.47$	-0.876 ± $j3.12$
-4.28	-17.88.

The corresponding asymptotic response is shown in Fig. 13. The complete circuit is shown in Fig. 14.

The low-frequency response of the circuit of Fig. 14 is controlled by the input transformer T_1 , the interstage transformer T_2 , and by-pass capacitors C_4 and C_5 . Very important also is the low-frequency performance of the regenerator output transformer. The components chosen produce a net effect of a 2-kc break due to T_1 cutoff, another 2-kc break due to T_2 and C_4 and C_5 (an approximation) and a 16-kc cutoff due to the regenerator output transformer. The low-frequency transfer function is then

$$L(s) = \frac{s^3}{(s + 0.01)(s + 0.0012)(s + 0.0012)} \quad (27)$$

with s again in units of 10^7 radians per second. The preamplifier transfer function is then (including effect of regenerator output transformer)

$$A(s) = K_v(s)L(s) \quad (28)$$

and is plotted (excluding effect of regenerator output transformer) in Fig. 15. It was planned that a filter ahead of the preamplifier would remove the higher lobe of response. However, the presence of the lobe is not sufficiently injurious to merit the cost of the filter.

Measured upper-frequency open loop gain and phase is shown in Fig.

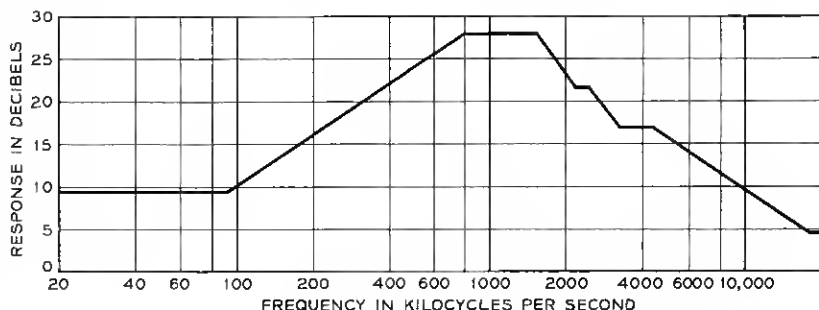


Fig. 13 — Asymptotic response of K_v .

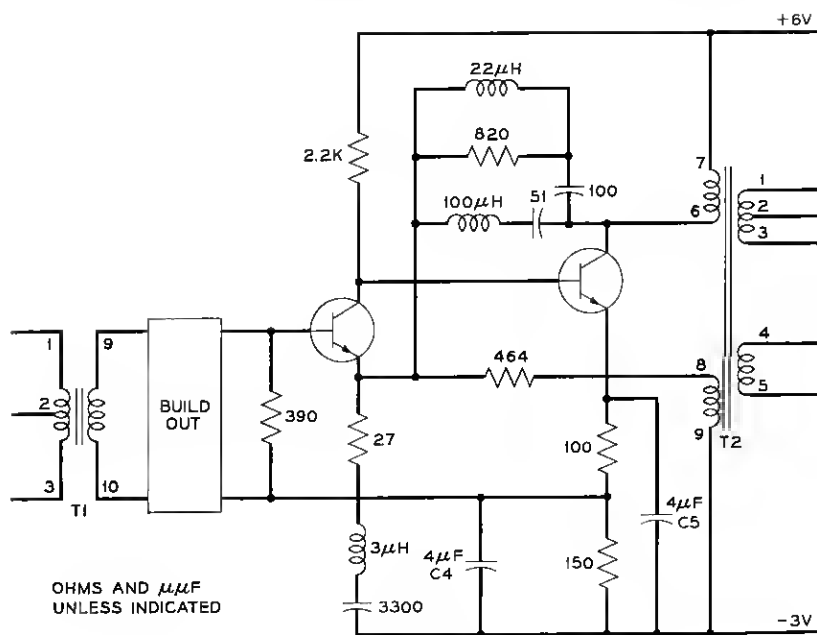


Fig. 14 — Repeater preamplifier circuit.

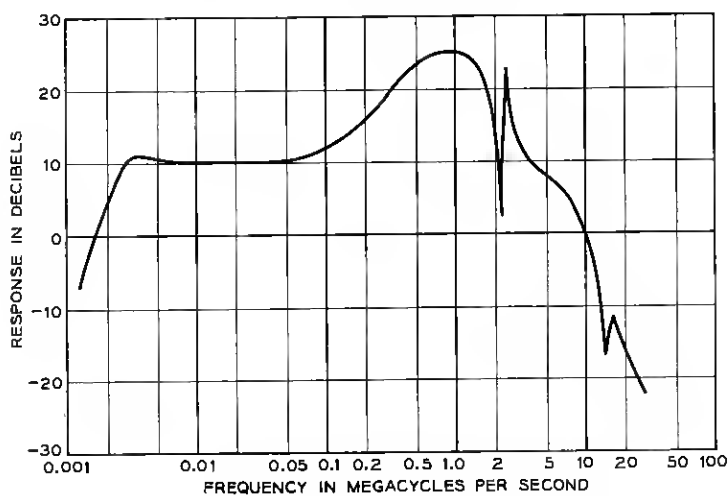


Fig. 15 — Measured preamplifier response.

16. The phase margin (36 mc) is 70° , and there is no phase crossover of 180° in the range of the measurement. For the by-pass capacitors used, the system is stable at low frequencies also, for all transistor gains from zero to infinity.

The equalized transmission medium from regenerator to decision point is

$$G(s) = C(s)K_v(s)L(s). \quad (29)$$

The measured response from line input (not including the effect of regenerator output transformer cutoff) to preamplifier output at pins 1 and 2 of T_2 is shown in Fig. 17.

4.2.2 Time Response

Response of $G(s)$ to a 50 per cent duty cycle, 1.5-mc rectangular pulse is shown in Fig. 18. The measured pulse is seen to be quite asymmetrical with a tail that is 20 per cent of the peak pulse height, one time slot after the peak. The difference between computed and measured response is attributed primarily to the poor analytical representation of the cable, (8).

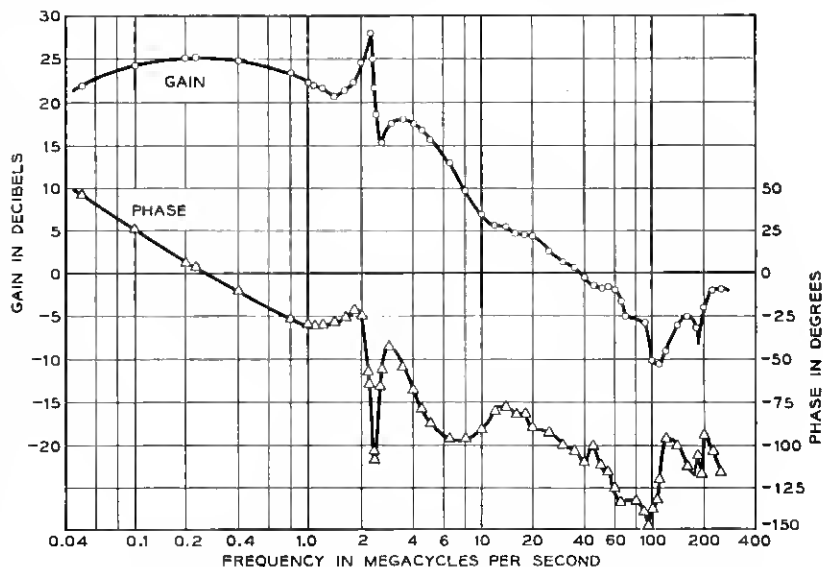


Fig. 16 — Measured open-loop transmission of repeater preamplifier.

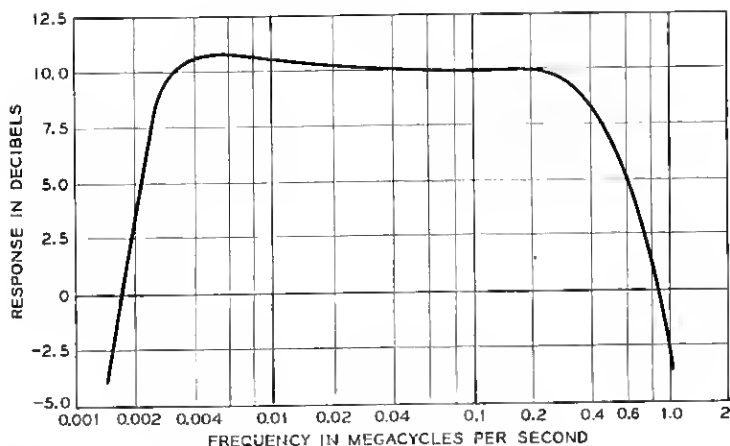


Fig. 17 — Approximate over-all response (not including regenerator output transformer).

Examining Fig. 18, one naturally asks: What can be done to further improve the signal-to-crosstalk situation? There appears to be as much as several db (additional allowed crosstalk coupling) available by improved equalization. Most of this may be obtained without field equalization adjustment by a very simple nonlinear equalizer.

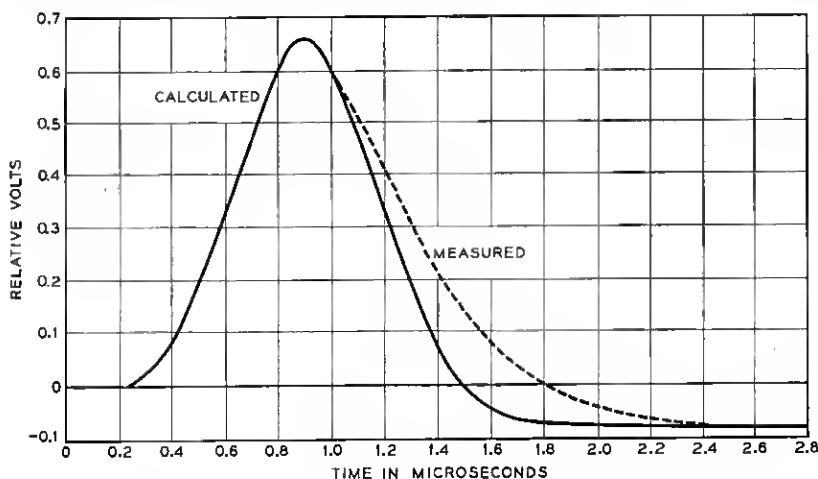


Fig. 18 — Response of line plus preamplifier to a 0.324-microsecond pulse.

4.2.3 Nonlinear Equalization

Special transmitted pulse shapes may be used to reduce intersymbol interference. The shape may be adjusted to optimize a decreasing intersymbol interference-increasing peak crosstalk interference situation. An example of such transmission is bipolar-dipulse,* which may be sent directly over the unequalized cable (or an ideal integrator) and which produces received pulse shapes that are almost completely resolved to one time slot. One can interpret the action of the two halves of the dipulse as a mark-crash operation that may not be so critical of the exact nature of the transmission medium. A similar but different preshaping will be considered and will be referred to as nonlinear equalization because of the way it is derived, and, as applied, has other nonlinear effects.

Assume a blocking oscillator is operating into an inductive load as shown in Fig. 19. The effect of the inductive load, in conjunction with the

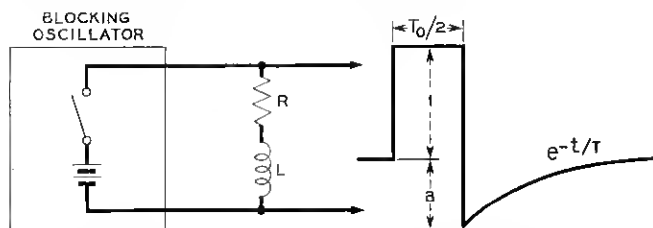


Fig. 19 — Simplified blocking oscillator operating into inductive load.

nonlinear blocking oscillator output impedance is equivalent to a "black box" transfer characteristic

$$Y_2(s) = 1 - \frac{a s e^{-(sT_0/2)}}{\left(s + \frac{1}{T}\right) (1 - e^{-(sT_0/2)})} \quad (30)$$

where a is the amplitude of the afterkick and T is the decay time constant. It is convenient if the afterkick is assumed to be of rectangular form of duration $T_0/2$ with an area equal to the actual afterkick area, a fair approximation in a severely band-limited medium. The transfer function becomes

$$Y_3(s) = 1 - \bar{a} e^{-(sT_0/2)} \quad (31)$$

* Achieved by passing bipolar signals through $\left(1 - \exp \frac{-sT_0}{2}\right)$.

where

$$\bar{a} = \frac{2a}{T_0} \int_0^{\infty} e^{-(t/T_0)} dt = \frac{2aT}{T_0}. \quad (32)$$

Let $g(t)$ represent the actual received pulse of Fig. 18. The effect of (31) may be added in the time domain. If T_m is the time of the pulse peak, and if the afterkick does not materially shift the position of this peak, the received pulse amplitude becomes

$$A_{\max} = g(T_m) - \bar{a}g\left(T_m - \frac{T_0}{2}\right). \quad (33)$$

And the height of the tail of the new pulse, one time slot after the peak, is

$$I_T = g(T_m + T_0) - \bar{a}g\left(T_m + \frac{T_0}{2}\right). \quad (34)$$

The crosstalk path is highly differentiative, so the peak crosstalk interference is approximately proportional to the height of the largest voltage transition of the transmitted pulse. Therefore, letting $N(t)_{\max}$ represent the new peak interference,

$$N(t)_{\max} = n(t)_{\max} (1 + \bar{a}). \quad (35)$$

Reading from Fig. 18,

$$g(T_m) = 0.65 \quad (36)$$

$$g\left(T_m - \frac{t_0}{2}\right) = 0.30 \quad (37)$$

$$g\left(T_m + \frac{t_0}{2}\right) = 0.40 \quad (38)$$

$$g(T_m + t_0) = 0.10. \quad (39)$$

Thus

$$A_{\max} = 0.65 - 0.30 \bar{a} \quad (40)$$

$$I_T = 0.10 - 0.40 \bar{a} \quad (41)$$

$$N(t)_{\max} = n(t)_{\max} (1 + \bar{a}). \quad (42)$$

One observes that I_T decreases faster with \bar{a} than $N(t)_{\max}$ increases with \bar{a} . The optimum \bar{a} is then that which reduces I_T to zero

$$\bar{a}_{\text{opt}} = \frac{0.1}{0.4} = 0.25. \quad (43)$$

The half height of the eye, h , is approximately $\frac{A_{\max}}{2} - I_r$,

$$h = \frac{0.65}{2} - 0.1 = 0.225, \quad \bar{a} = 0 \quad (44)$$

$$\bar{h} = \frac{0.58}{2} - 0 = 0.290, \quad \bar{a} = 0.25 \quad (45)$$

If 25 per cent of the received pulse height is allotted to other degradations, the allowed peak crosstalk,

$$n(t)_{\max} = 0.75 \left(\frac{A_{\max}}{2} \right) - I_r \quad (46)$$

$$n(t)_{\max} = 0.75 \left(\frac{0.65}{2} \right) - 0.1 = 0.142, \quad \text{for } \bar{a} = 0 \quad (47)$$

$$n(t)_{\max} = 0.75 \left(\frac{0.58}{2} \right) - 0 = 0.218, \quad \text{for } \bar{a} = 0.25. \quad (48)$$

But the actual $N(t)_{\max}$ for $\bar{a} = 0.25$ is

$$N(t)_{\max} = 0.142(1 + 0.25) = 0.178. \quad (49)$$

The new equalization thus allows additional crosstalk coupling to the extent of a factor of 2.18/1.78 or about 2 db.

The measured received pulse for $a = 0.25$ and $T = 0.3 \mu\text{sec}$ (values found experimentally to be optimum, considering all effects of the RL network) is shown in Fig. 20. The corresponding \bar{a} is given by (32)

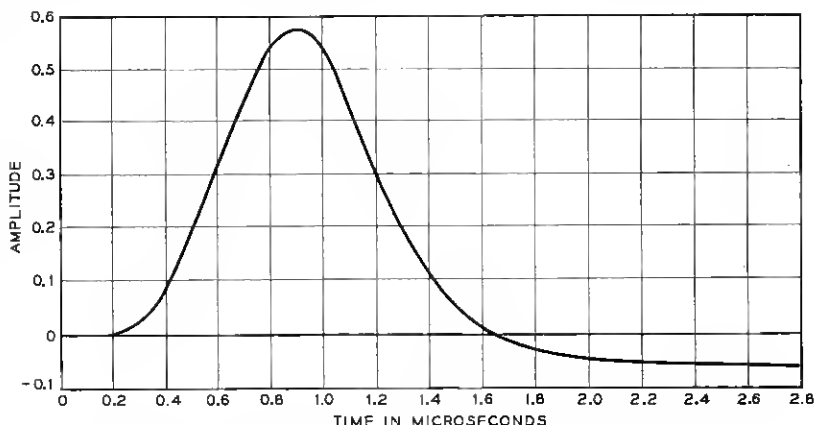


Fig. 20 — Pre-amplifier output including effect of RL network.

$$\tilde{a} = \frac{2(0.25)(0.3)}{0.628} = 0.24 \quad (50)$$

a value almost equal to that expected considering the effect of the network on equalization alone.

4.3 Line-Build-Out Networks

The nature of PCM transmission is such that small variations in received pulse shape may not be consequential. A field equalization adjustment dependent upon the exact length of a particular section of cable does not appear justified. An attractive proposal is to build out any line length by means of one of a quantized set of networks to an equivalent 6000 feet plus or minus some quantization error.

The build-out network is a separable option on the repeater and, for many reasons, should be a simple network. A single-break-frequency network is desirable, and is a good approximation when the cable length

TABLE III — BUILD-OUT NETWORK PARAMETERS

Build-Out Network (feet)	Flat Loss (db)	Corner Freq. (kc)
5000	4.0	90
4000	3.0	120
3000	3.0	250
2000	1.5	340
1000	1.2	700

to be simulated is small. For shorter-spaced repeaters, a poor approximation is satisfactory, for little margin must be allotted to interference.

A bridged-*T* network has the desirable feature that flat-loss and break-frequency may be controlled independently. In the vicinity of central offices, the over-all transmission frequency band may be increased and flat loss adjusted to further open the eye, yet maintain nominal received pulse level. An equalization optimization problem exists for each build-out. The optimization, however, is relative to a statistical quantity (allowed impulse noise), and is not so "sharp" as was the case for "fixed amplitude" NEXT. Very nearly optimum LBO's result if the transmission band is limited to produce only slight intersymbol interference. A set of resulting loss and corner frequency values is given in Table III.

Using the $C(s)$ of (8) and the preamplifier characteristic of (28) produces the amplitude versus cable length curve of Fig. 21.* One thousand

* The actual computation was based on an amplifier characteristic slightly different from (28) and a better approximation to the cable characteristic than (8). The effect of the RL equalizer was not included. It is felt, even so, that the amplitude-line length function obtained is in close agreement with that available from (28), (30) and (8).

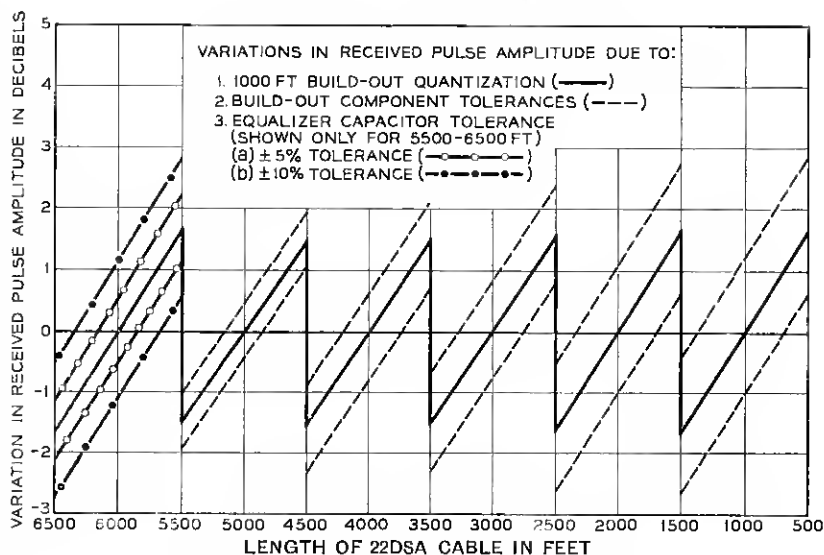


Fig. 21 — Variations in amplitude vs cable length.

foot build-out quantization is seen to contribute about 3 db to the expected variation in received pulse height. Five per cent component tolerances in the LBO network contribute a maximum gain variation of 0.5 to 1 db, depending upon length of cable represented. A 5 per cent variation in C_2 of the amplifier contributes another 0.5 db to variation in received pulse height.

V. VOLTAGE CROSSHAIR

In a severely band-limited system, the received pulse amplitude is dependent upon both width and height of the transmitted pulse. In addition, variations in line loss, line-build-out parameters, and amplifier characteristics affect the received pulse amplitude (and shape). A realizable set of variations is shown in Table IV.

A 3-to-1 variation in received pulse amplitude is thereby expected, aerial operation being accommodated by better LBO control (twice as many networks). To materially reduce this variation in received pulse amplitude requires components of extreme tolerances. Even a field gain adjustment to eliminate items 3, 5, 6, 7 would leave a total variation of 5 db for underground and 8 db for aerial operation. A field gain adjustment can also eliminate items 1 and 2, but this requires adjustments at three locations each time a two-way repeater is replaced. Item 4 alone accounts for 2 db and 5 db for the two types of plants. In a repeater

TABLE IV — FACTORS AFFECTING RECEIVED PULSE HEIGHT

Factor	Manhole 32-100°F	Aerial -40 to +140°F
1. Pulse height.....	±1.0 db	±1.0 db
2. Pulse width.....	±0.5 db	±0.5 db
3. Line loss (3 σ limit).....	±1.0 db	±1.0 db
4. Line loss (temp.).....	±1.0 db	±2.5 db
5. LBO Quantization.....	±1.5 db	±0.7 db
6. LBO Parameters.....	±1.5 db	±0.8 db
7. Preamp characteristic.....	±0.5 db	±0.5 db
Total.....	±7.0 db	±7.0 db
Items 4 + 5 + r.s.s. of others.....	±4.7 db	±4.9 db

with a fixed threshold at one half the nominal received pulse height, a loss of 1 db in pulse height results in a 2-db penalty in crosstalk performance. A 2.5-db loss of amplitude produces a 5-db penalty.

How should level control be implemented? There are two important approaches, automatic gain control and automatic threshold control. Automatic gain control is most desirable for it maintains fixed preamplifier output, which in turn prevents line and gain variations from affecting recovered clock level. But automatic gain control is rather difficult to realize, requiring a voltage-sensitive device, making it generally expensive and difficult to maintain linearity. It is, however, rather easy to obtain a voltage proportional to received pulse height, and this voltage may be used as the detection voltage crosshair. This simplicity gives automatic threshold control a decided advantage over automatic gain control. Variation in clock level with transmission gain is not too consequential, for it varies violently with pattern anyway.

5.1 Realization

Fig. 22 shows a possible implementation of automatic threshold control. A balanced preamplifier output delivers hipolar pulses to two decision gates. Assuming the transistor base-emitter drop V_{BE} equals the diode forward drop, regenerator R_1 works when the output "a" exceeds ground, and R_2 works when output "b" exceeds ground. A negative voltage V_c applied at c allows R_1 to work when the preamplifier output $v_o > V_c$, and R_2 works when $v_o < -V_c$. Thus the threshold voltage at c is applied to both pulse polarities, and the hipolarity of the signal is automatically maintained through the regenerator.

The proper "threshold voltage," $|V_c|$, is achieved by setting the turns ratio of the preamplifier output transformer and selecting V_R such that it cancels the peak-detecting diode drop. Capacitor C_6 is large enough to make V_c a slow function of time, able to follow long-term variations but unable to vary between pulses.

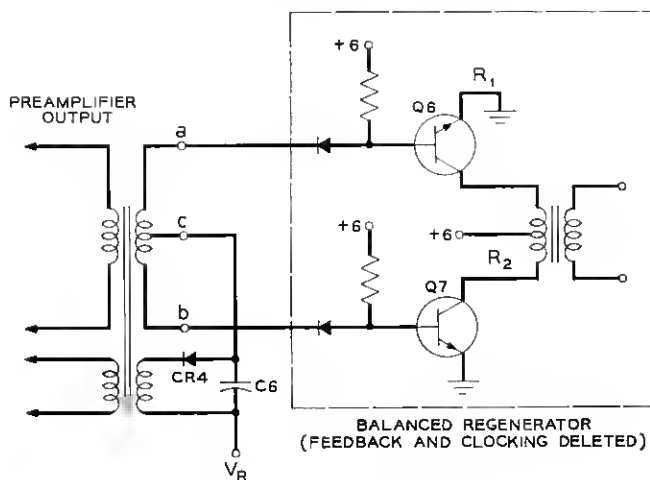


Fig. 22 — Conceptual threshold circuit.

Two changes are necessary to make the circuit workable. These are shown in Fig. 23. First the peak-detecting diode must be able to carry the average gate current. Peak diode current is approximately

$$I_P = \frac{I_{gate}}{\tau} \quad (51)$$

where τ is an equivalent fractional conduction time for the diode. If the drop across the diode is not to exceed 8 per cent of V_c , Fig. 20 shows the conduction time to be approximately $0.200 \mu\text{sec}$. For minimum density pattern of 1 out of 8

$$I_P = \frac{I_{gate}}{\frac{200}{648} \times \left(\frac{1}{16}\right)} = 52 I_{gate}. \quad (52)$$

The preamplifier is not likely to be able to deliver this peak current, so dc gain must separate the peak detector and gate. This is the function of Q_3 in Fig. 23.

Secondly, consideration must be given to the noise performance of the peak rectifier. In Fig. 22 the charging time constant for C_6 is much less than the discharge time constant. A short burst of noise may charge C_6 to an extreme value, producing a long tail of repeater errors after the disturbance. In Fig. 23, C_6 is chosen small and C_9 as large as economical and R_{15} as large as allowed. Selection of the proper time constants for the threshold circuit depends upon the nature of the interference, the over-

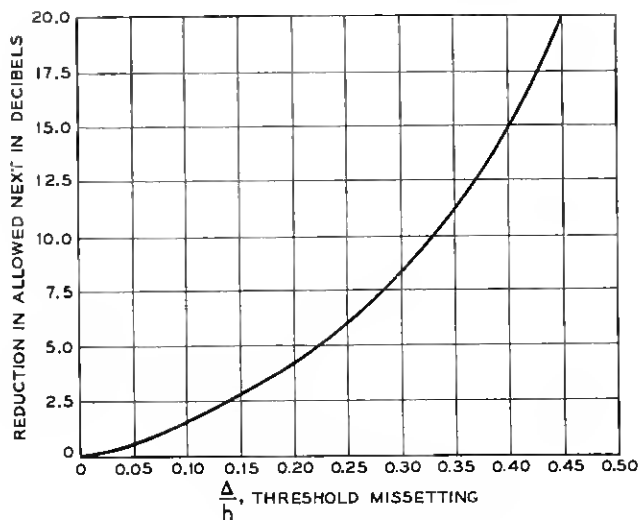


Fig. 24 — Reduction in allowed NEXT as a function of threshold mis-setting in fraction of height of eye.

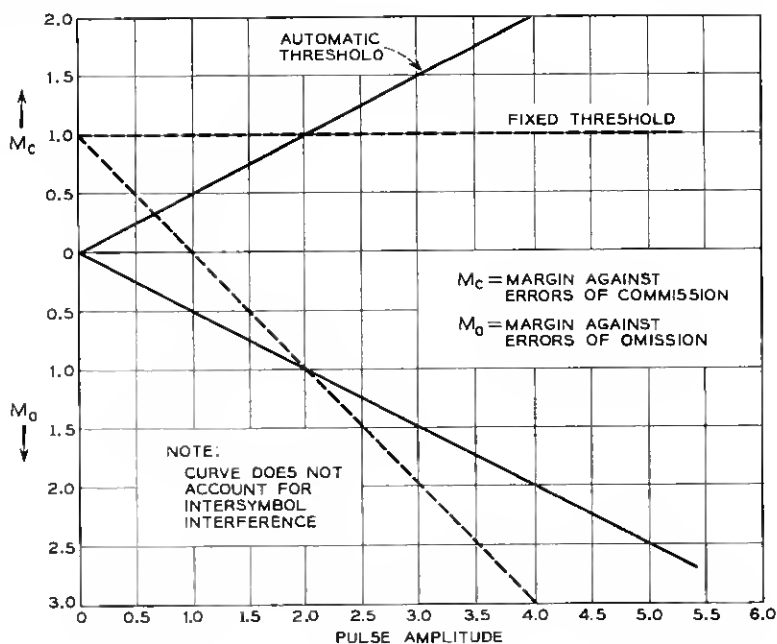


Fig. 25 — Relative margin against errors as a function of received signal amplitude.

where

V_{BEX} = "just conduct" base-emitter voltage of Q_6 or Q_7

$V_f(I_0)$ = diode forward drop

V_{BEY} = base-emitter drop of Q_3

I_c = collector current of Q_3

β_0 = dc common emitter gain of Q_3 .

But V_{BE} , V_f and β_0 are statistical quantities, and V_R can be selected only to satisfy (54) for nominal parameter values. With that V_R , however, reasonable transistor and diode specifications make the left-hand side of (54) as large as ± 375 millivolts, which for a 2-volt eye is a 4-db penalty in allowed peak interference (Fig. 24). A factory adjustment of each repeater is called for, but the expense, size, and unreliability of a potentiometer do not seem justified. A satisfactory solution is a strapping option made at time of factory checkout. V_R is selected for nominal device voltage drops. One strap option raises V_R by 0.25 volt, another strap lowers V_R by 0.25 volt. The resulting threshold placement is correct to within 0.125 volt. Furthermore, since the deviation is due to many device parameters, extreme deviations should seldom be encountered, so most repeaters should come out with option 1, no strap at all.

Temperature dependence of the threshold voltage is primarily through the dependence of β_0 of Q_3 . The diode and transistor drops around the threshold loop generally "track" with temperature. However, any change in Q_3 base current produces a voltage drop in R_{15} and R_{16} . The variation in this drop for $\beta_0 = 20$, $\beta_{\text{min}} = 12$ and $\beta_{\text{max}} = 50$, with $R_1 = 300$ ohms $R_2 = 470$ ohms and $I_c = 10$ ma, is approximately ± 0.25 volt, a worst case. For higher initial β_0 's, the situation is not so severe.

5.2 Effect of NEXT

The effect of NEXT on the automatic threshold is interesting. There are many cases, but let us consider only the case of a single interferer which is only slightly asynchronous.

The threshold will then be set by the sum of the signal and crosstalk when both signal and interference peak fall in phase. When the crosstalk is out of phase with the signal, the sum signal has peaks no higher than the desired signal alone. There thus appears a beat-frequency component in the threshold circuit equal to the height of the interference. If the bit rates of the two signals differ considerably, the low-pass filter in the threshold loop will reduce the beat-frequency component.

Assuming the threshold interference voltage sinusoidal

$$V_c = r[E_m + \frac{1}{2}n(t)_{\max}(1 + \sin \Delta\omega t)] \quad (55)$$

where r is the fractional threshold setting.

Neglecting intersymbol interference, and letting M_c be the margin against errors of commission and M_0 be the margin against errors of omission, then

$$M_c = V_c - n(t)_{\max} \quad (56)$$

$$M_0 = E_m - n(t)_{\max} - V_c \quad (57)$$

when V_c is a minimum, M_c is a minimum, and by (55) and (56)

$$(M_c)_{\min} = rE_m - n(t)_{\max} \quad (58)$$

when V_c is a maximum, M_0 is a minimum, and

$$(M_0)_{\min} = (1 - r)E_m - (1 + r)n(t)_{\max}. \quad (59)$$

The optimum r allows M_c and M_0 to simultaneously go to zero as $n(t)_{\max}$ increases. When

$$(M_c)_{\min} = (M_0)_{\min} = 0 \quad (60)$$

$$n(t)_{\max} = rE_m = \frac{1 - r}{1 + r}E_m \quad (61)$$

$$r = 0.414. \quad (62)$$

For the case considered, the effect of $n(t)$ on the threshold voltage requires, for optimum performance, that the voltage crosshair be set at 41.4 per cent of the peak received signal. Optimum setting for a fixed threshold voltage (for the assumptions made) would be at 50 per cent of the received signal.

The automatic crosshair positioning thereby potentially introduces up to a 1.6-db penalty in crosstalk performance. All of the 1.6 db is not lost in a practical repeater because, for example, $n(t)_{\max}$ must be less than $0.5 E_m$, especially due to intersymbol interference, and the special case considered is highly idealized in many other respects.

VI. TIME CROSSHAIR

The equalized and amplified pulse shape shown in Fig. 20 can be crudely matched by

$$c(t) = 1 + \cos \frac{\pi t}{T_0}. \quad (63)$$

Peak crosstalk interference is given by something between the (1.0,5) and (1.25,4) entries of Table II. The measured quantity is almost in the center of this range, 0.18,

$$n(t)_{\max}(10^{-9})(k^{-1}) = 0.18 \quad (64)$$

and by (17)

$$n(t)_{\max} = 0.18(10^{-(x-40)/20}). \quad (65)$$

Fig. 26 is a plot of (65) and shows the peak crosstalk at the decision point as a function of crosstalk loss. Contours of constant x may now be drawn on the eye diagram by adding the corresponding $n(t)_{\max}$ to the Case 1, Case 2 curves, and subtracting $n(t)_{\max}$ from the Case 3 curve. Fig. 27 results. The eye is seen to close at $x = 31.5$ db. At $x = 34$ db, the time crosshair must be held within $\pm 0.108 \mu\text{sec}$ minus the crosshair half-width.

6.1 Effect of Clipping Level

As previously stated, clock may be recovered from a bipolar pulse train by rectification of the received signal. For various reasons, a primary one being the elimination of adverse pattern conditions in near-end crosstalk, the received pulses are clipped to about half amplitude by the clock rectifier. This eliminates interference on the pulse train baseline and resolves the pulses to their own time slot. However, the clipping operation affects both the amplitude and phase of the recovered clock.

Empirically, the variation of phase of the recovered clock with clipping level is shown in Fig. 28(a), and the variation of clock amplitude with clipping level is shown in Fig. 28(b). As a compromise between phase variation with pattern and loss of amplitude, and because it is

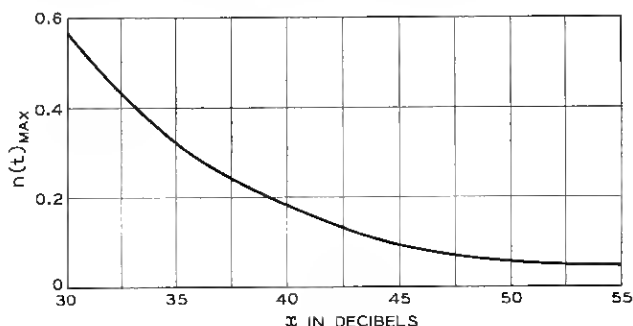


Fig. 26 — Peak crosstalk interference as a function of 1.544-mc crosstalk loss.

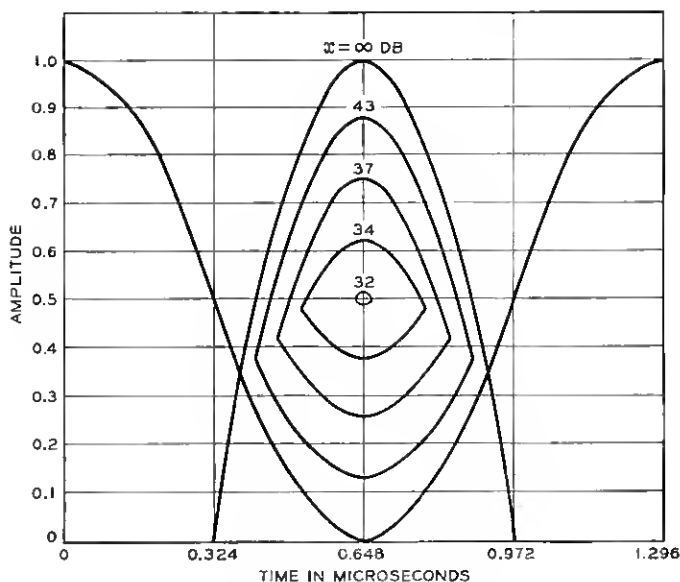


Fig. 27 — Eye size for various values of NEXT loss.

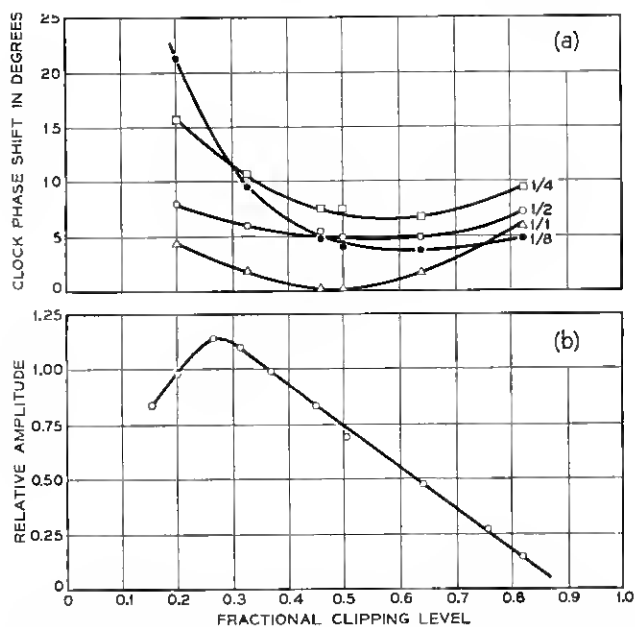


Fig. 28(a) — Measured clock phase as a function of clipping level for various patterns; (b) measured clock amplitude as a function of clipping level for 4/8 pattern.

very easy to implement, the clock clipping level may be set by the voltage crosshair signal to approximately half the peak received pulse. This produces an expected pattern jitter of 6° , and a nominal clock phase that varies 3° as the clipping level is varied ± 10 per cent from half-peak amplitude (for an average pattern such as $\frac{4}{8}^*$).

6.2 Effect of Width

The time crosshair is subject to jitter due to timing interference via near-end crosstalk. Assuming the timing signal is transmitted at 772 kc, (8) gives

$$20 \log |C(j2\pi \cdot 772 \text{ kc})| = -30 \text{ db} \quad (66)$$

and by (5) and (16)

$$20 \log \frac{H(S)}{A(S)} = -(x + 6) \text{ db}. \quad (67)$$

The signal-to-noise in the timing channel is then, due to crosstalk interference,

$$20 \log S/N = -30 + (x + 6) = x - 24 \text{ db}. \quad (68)$$

A word about the assumed 772-kc timing. The assumption holds almost exactly for $a_j = b_j = 1$ (full pattern); it fails considerably for some particular patterns. For random patterns, it is a fair approximation. The S/N ratio quoted is then, at best, a fair approximation. The maximum clock jitter for any $S/N < 1$

$$j_{\max} = \sin^{-1} \frac{N}{S} \quad (69)$$

$$j_{\max} = \sin^{-1} [10^{-(x-24)/20}], \quad x > 24 \text{ db}. \quad (70)$$

Fig. 29(a) is a plot of (70). The eye closes when $j_{\max} \approx 25^\circ$. The allowable jitter is

$$J(x) = \frac{W(x) - \delta - 2\epsilon}{2} \cdot \frac{360}{0.648} \quad (71)$$

where

$W(x)$ = eye width in presence of crosstalk in μsec

δ = crosshair width in μsec

ϵ = deviation of crosshair from optimum placement, in μsec .

* n/m will be used to indicate repetitive words of m time slots, each with n consecutive pulses in the word.

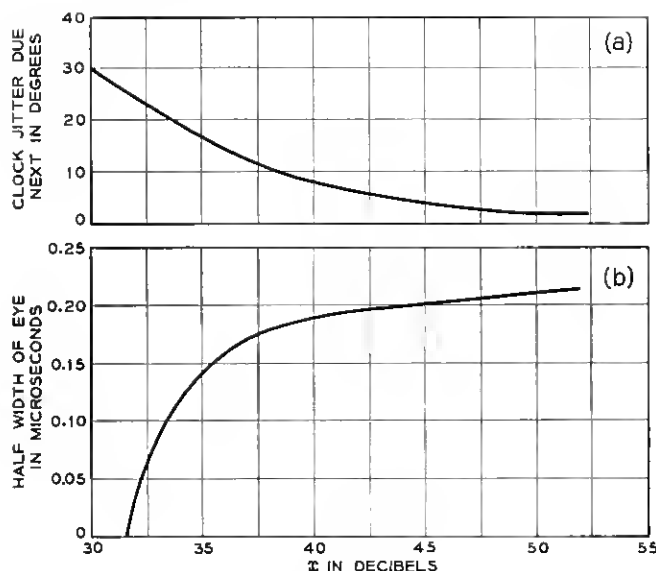


Fig. 29 — Clock jitter (a) and half width of eye (b) as a function of 1.544-mc NEXT loss.

$W(x)$ is available from Fig. 27 and is plotted in Fig. 29(b). Equating $J(x)$ to j_{\max} , one obtains the minimum allowable crosstalk loss as a function of sample width.

$$\frac{360}{0.648} \cdot \frac{W(x) - \delta - 2\epsilon}{2} = \sin^{-1}[10^{-(x-24)/20}]. \quad (72)$$

For each x one may read $W(x)$ from Fig. 29 and compute δ from (72). Fig. 30 results, which can be interpreted as the minimum crosstalk loss as a function of crosshair width. In reality, $\epsilon = 0$ cannot be maintained; $\epsilon = 0.054 \mu\text{s}$ ($\pm 30^\circ$) is realistic. One concludes that, for $\epsilon = 30^\circ$, a crosshair width of $0.1 \mu\text{s}$ is reasonable. The penalty in crosstalk performance for this finite width is about a db.

6.3 Timing Extraction

Many circuits for clock extraction were considered, and three circuits were reduced to hardware. The preferred circuit (adequate performance at minimum cost) has a single LC tank for clock extraction. Automatic phase-locked oscillator and crystal tank circuits, while workable and possessing certain desirable features, require all the components of the

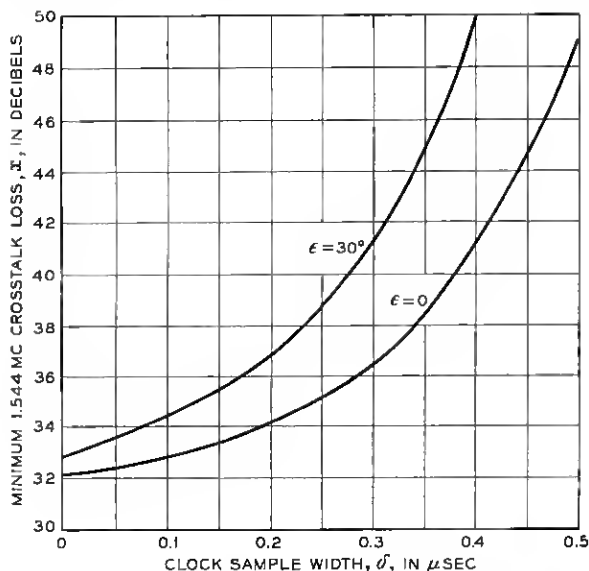


Fig. 30 — Minimum crosstalk loss as a function of crosshair width.

LC tank plus others. Stability requirements on the LC tank are lessened in the latter two approaches. (The phase-locked oscillator developed uses an LC tank in the oscillator; the damped crystal works into an LC tank.) The crystal tank is particularly difficult because of the poor phase stability of a crystal and the difficulties in compensating for crystal shunt capacitance.

The effective Q of the timing circuit must be large enough that (1) the timing circuit can bridge gaps between pulses in the received train and such that (2) the phase of the recovered clock varies with pulse pattern in an acceptable manner. The better resolved the received pulses, the smaller the pattern shift. Generally, bandwidth and gain limitations result in an unresolved pulse driving the timing circuit. Separate equalization for the clock path does not seem justified for, with a clock Q of 50 to 100, a maximum pattern shift of 10° per repeater appears tolerable and realizable.

The effective Q of the timing circuit must be small enough that over the temperature range (-40 to $+140^\circ\text{F}$) and 20-year life, the phase of the clock is stable to $\pm 30^\circ$ (1 db crosstalk penalty). It will be seen that the time crosshair can be placed only to the nearest $\pm 10^\circ$, so that only $\pm 20^\circ$ are available for temperature and aging. With minimum Q 's of

75 and maximum Q 's of 100, the required stability in resonant frequency is

$$\pm \tan 20^\circ \geq 2Q \frac{\Delta f}{f} = 200 \frac{\Delta f}{f} \quad (73)$$

$$\frac{\Delta f}{f} \leq \pm 0.0018 \quad (74)$$

or the total allowed component variation is 0.36 per cent.

A carbonyl iron inductor is expected to age ≤ 0.1 per cent over a 20-year life. Tests on tubular ceramic capacitors show an aging trend of < 0.1 per cent over a 20-year life. The allowed temperature mistracking (-40 to ± 140) is then ± 0.16 per cent. Temperature coefficient of carbonyl iron is typically 0.6 per cent ± 0.3 per cent over the temperature range; a realizable capacitor (-0.6 per cent ± 0.3 per cent) produces an over-all coefficient of $+0.6$ per cent to -0.6 per cent over the range -40 to $+140^\circ\text{F}$. Initial tuning is done at midrange temperature, so the expected over-all variation is $< \pm 0.3$ per cent, almost double the requirement of ± 0.16 per cent. It is not likely that both inductor and capacitor will age in the wrong direction by the maximum amount and individually have worst-case temperature coefficients that aid the aging effect. If this should happen, the clock phase will be off as much as

$$10^\circ + \tan^{-1}[200(0.25 \times 10^{-2})] = 36.6^\circ. \quad (75)$$

This additional shift increases the minimum crosstalk loss by another db. The situation as presented appears workable but is pushing the art of component stability.

6.4 Implementation

The clock circuit must accept pulses of heights from 1 to 3 volts, clip off the bottom half of the pulse, and from this pattern-varying train deliver a stable uniform clock to the regenerator.

For a full-pulse pattern, the clipped signal delivered to the tuned tank is very nearly a rectified sine wave of 0.5 volt minimum amplitude. The 1.544-mc component is $4/3\pi \times 0.5$ or 0.212 volt. The minimum density level (1 out of 8 pulses present) is about $(1/8)(0.212) = 0.0265$ volt. The maximum signal is $3 \times 0.212 = 0.636$ volt. The clock amplitude thus varies over a 28-db range, and the clock circuit must clip this back to a constant-level signal, yet introduce no appreciable amplitude-to-phase conversion.

Two LC clock circuits have been built. Both have a gated output stage.

One has a two-transistor feedback amplifier driving the output stage, with limiting in the feedback path. The other is forward-acting with diode clipping. The latter circuit is shown in Fig. 31.

The automatic threshold voltage serves as a clipping voltage for the clock. An emitter follower provides a low driving impedance for the tank (the dc gain of this transistor is used in the automatic threshold circuit). A phase shifting stage with current feedback drives a switched output stage.

6.4.1 Effective Q

The effective Q of the tank circuit, Q_c , is given by

$$\frac{1}{Q_c} = \frac{1}{Q_s} + \frac{1}{Q_T} + \frac{1}{Q_L} \quad (76)$$

where

Q_s = source Q

Q_T = tank Q

Q_L = load Q

The source Q is controlled by the output impedance of Q_3

$$Q_s \approx \frac{\omega_0 L}{R_s \left[\frac{C_s}{C_7 + C_8 + C_{15}} \right]^2} \quad (77)$$

where R_s is given by

$$\frac{1}{R_s} = \frac{1}{R_9} + \frac{1}{R_0} \quad (78)$$

where

$$R_0 = r_e + \frac{r_b' + R_p}{1 + \beta}, \quad R_p \approx \frac{R_{16} \times R_{19}}{R_{16} + R_{19}}, \quad (79)$$

r_e , r_b' , and β are conventional parameters of Q_3 , and L is the full inductance of T_4 . R_s is about 15 ohms for the minimum allowed β (≈ 20), so for the parameters of Fig. 31

$$Q_s \approx 270. \quad (80)$$

The tank Q is controlled by many factors. Carbonyl iron possesses the required stability, and the resulting Q_T is quite dependent on inductor size. Three inductor sizes were developed, all 100- μ henry coils. The larger

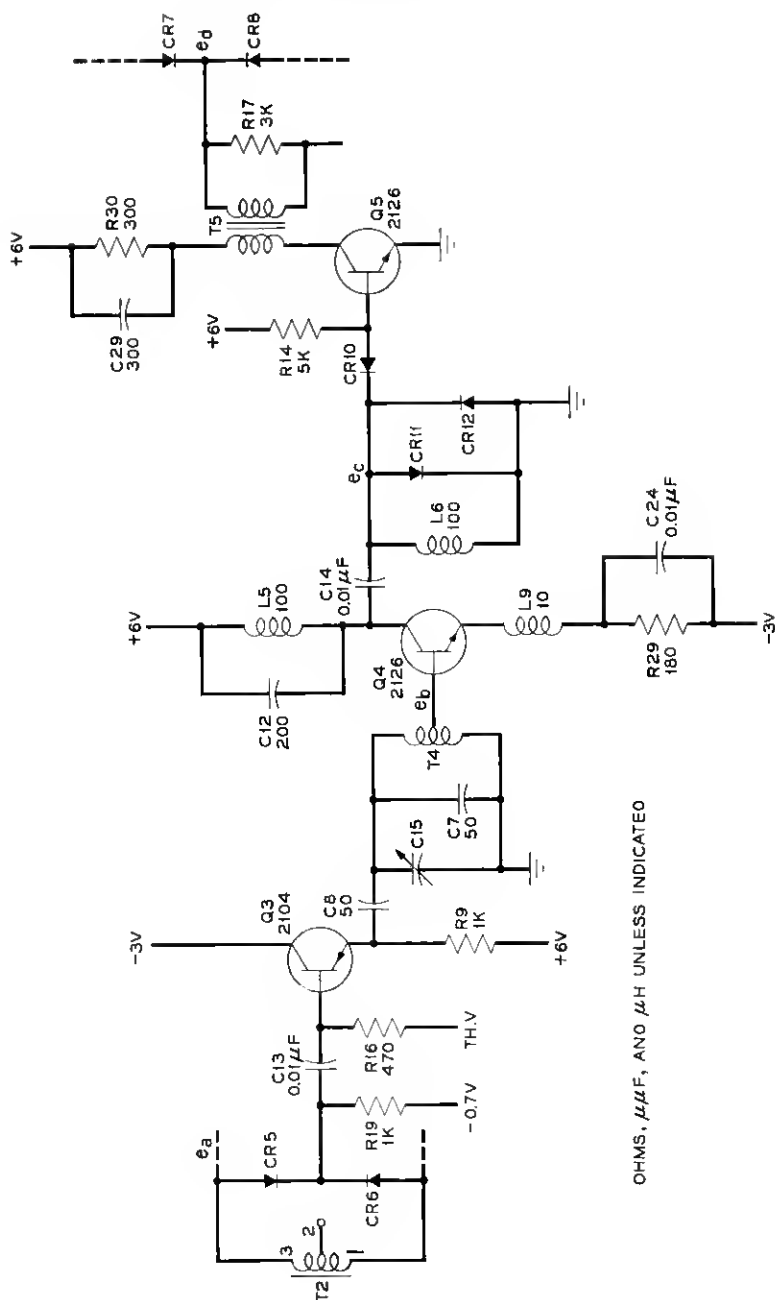


Fig. 31 — Repeater clock circuit.

inductor has $Q_T \approx 200$; the intermediate size inductor has $Q_T \approx 150$; and the smaller inductor has $Q_T \approx 100$. The intermediate size was selected to give an over-all circuit Q of 75–100.

The load Q is controlled by R_i , the input resistance to Q_4

$$\frac{1}{R_i} = \frac{1}{\omega_\beta \beta_0 L_9} + K \omega_0 C_c \quad (81)$$

where

ω_β = common emitter cutoff frequency of Q_4

β_0 = low-frequency common emitter gain of Q_4

K = voltage gain of Q_4

C_c = collector capacity of Q_4 .

The first term represents a conductance of about 0.1 millimho and the second term a conductance that may vary with signal level from about 0.2 millimho to almost zero. The load Q becomes

$$Q_L = \frac{n^2 R_i}{\omega_0 L} \quad (82)$$

With $n = 10$, for nominal signal levels $Q_L > 330$.

The resulting minimum effective Q is approximately

$$\frac{1}{Q_c} = \frac{1}{270} + \frac{1}{150} + \frac{1}{330} \quad (83)$$

$$Q_c = 75. \quad (84)$$

6.4.2 Gain

The voltage gain of the tank is

$$\frac{e_0}{e_i} \approx j \left(\frac{C_8}{C_7 + C_8 + C_{15}} \right) Q_c, \quad \text{for } Q_c \gg 1. \quad (85)$$

Using the parameters stated,

$$\frac{e_0}{e_i} = j3.75. \quad (86)$$

The signal delivered to the base of Q_4 is then in the range 0.1 to 2.3 volts peak. For random patterns with average line loss, the average level delivered to the base of Q_4 is about 1 volt peak.

A voltage gain of five in Q_4 brings the signal level up to the point where the input gate to Q_5 can be precisely operated. Clipping diodes

CR11 and CR12 limit the collector swing of Q_4 , which operates in its linear region for all signal levels.

One would expect a square wave of clock out of Q_5 . This would be true, except that the primary inductance of T_5 is selected small ($<60 \mu\text{henry}$) so that the transformer output overshoots measurably. This overshoot is used as the time crosshair for the regenerator input gate. The output of T_5 is then a three-level signal of shape shown in Fig. 32. The spike overshoot "initiates" the regenerator action and the negative excursion turns off the regenerator, thereby controlling regenerator output pulse width. T_5 must deliver enough current to rapidly shut the regenerator off; it must accept the gate current after the sample instant (if no received pulse is present), making the regenerator immune to any received signal changes that occur outside the sampling instant.

6.4.3 Clock Placement

The approximate phase relation of the clock signals is shown in Fig. 33. The clock spike is nominally centered in the "eye." The main sources of clock misplacement are:

i. Mistuning Effects

- | | |
|--------------------------------|-----------------------------|
| (a) LC temperature coefficient | $\pm 16^\circ \text{ max}$ |
| mistracking | |
| (b) LC aging | $\pm 11^\circ \text{ max}$ |
| (c) mistuning due source | $\pm 0.5^\circ \text{ max}$ |
| (d) mistuning due load | $\pm 6^\circ \text{ max}$ |

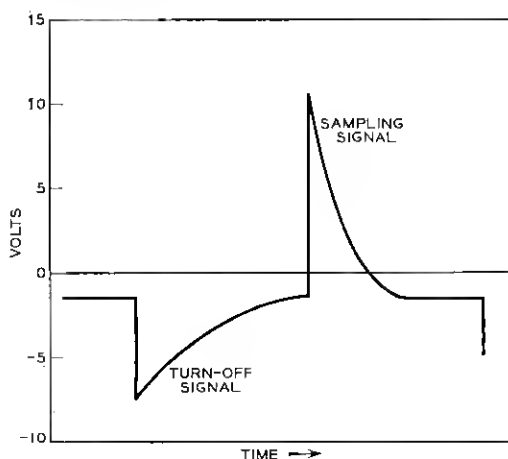


Fig. 32 — Idealized clock waveform.

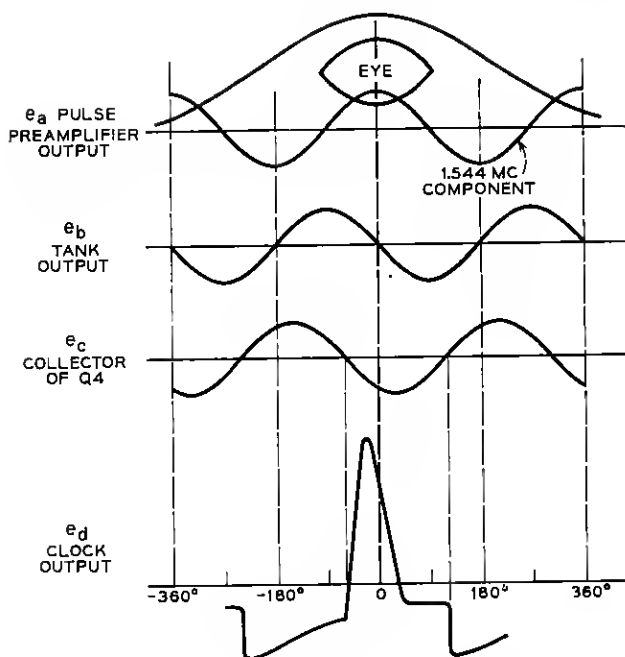


Fig. 33 — Clock phase at various points of Fig. 31.

ii. Placement Effects

(a) tolerances on L_5 , L_6 , C_{12} (5%)	$\pm 5^\circ$ max
(b) diode balance (CR_{11} , CR_{12})	0.5° max
(c) V_{BE} variation in Q_5	$\pm 8^\circ$ max
(d) storage time of Q_5	$\pm 5^\circ$ max

The effects under *ii* are additive; the effects under *i* can be added as long as the sum is small (directly on a $\Delta f/f$ basis). Direct addition gives $\pm 52^\circ$. An r.s.s. addition gives $\pm 23^\circ$. Most of the items under *ii* occur only for worst-case transistors and maximum line loss with minimum received clock, and are reduced considerably for reasonably random pulse trains. Clock position variations from nominal of the order of 20° to 40° should be expected, producing about a 1-db penalty in NEXT performance in accordance with Fig. 30.

VII. REGENERATOR

The regenerator design for a bipolar repeater is particularly governed by economic factors. Indeed, the requirement of a balanced regenerator is one that must be pondered before a decision against unipolar trans-

mission is made. On the other hand, of the four basic configurations, there is one, the shunt-series configuration, that allows a rather simple circuit. This arrangement, shown in Fig. 34, requires only one transformer, and the action of the feedback is such that one set of gate diodes may be used both for spike sampling and turn-off. For this configuration spike sampling comes "free."

Although in many ways advantageous, the shunt-series circuit has one outstanding disadvantage. Since the feedback windings are directly coupled to the transmission line, any line reflections are coupled into the feedback winding and become "noise" on the signal. The problem is aggravated by the fact that the regenerator is a poor termination for any reflected signal.

If ρ is the voltage reflection coefficient due to a discontinuity in the line

$$V_{\text{reflected}} = \rho V_{\text{incident}}$$

and if midband loss (5 db per 1000 feet) is assumed applicable, then the voltage coupled into the feedback winding is

$$V_{fb} \approx \frac{\rho(1 + \Gamma)}{3^{l-1}} \text{ volts} \quad (87)$$

for a 3-volt transmitted pulse, where l is the distance from repeater output to the discontinuity in kilofeet, and Γ the reflection coefficient the

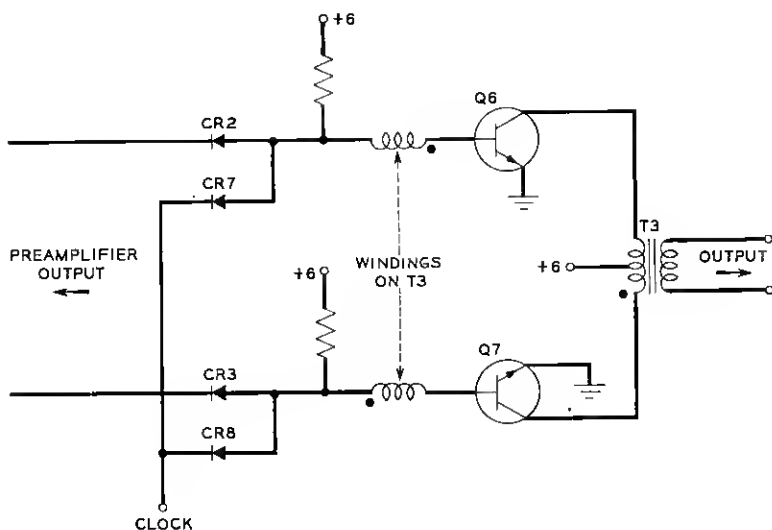


Fig. 34 — Regenerator circuit.

repeater output presents to the returned signal. It is planned that some matching will be provided by the coupling network to the fault-location system. Assuming a 1-volt eye half-height, V_{fb} reduces the allowable near-end crosstalk interference by

$$20 \log \frac{1}{1 - \frac{\rho(1 + \Gamma)}{3^{l-1}}} \quad (88)$$

a worse case occurring when the reflected signal peak occurs at the sampling instant. Equation (88) is plotted in Fig. 35. These curves vividly illustrate the gravity of line discontinuities close to a repeater output.

There are many ways to make the regenerator more tolerant or completely tolerant of line reflections, but all methods add to the cost. A small resistive pad between regenerator and line aids considerably. This can be inserted by either increasing output level, decreasing signal

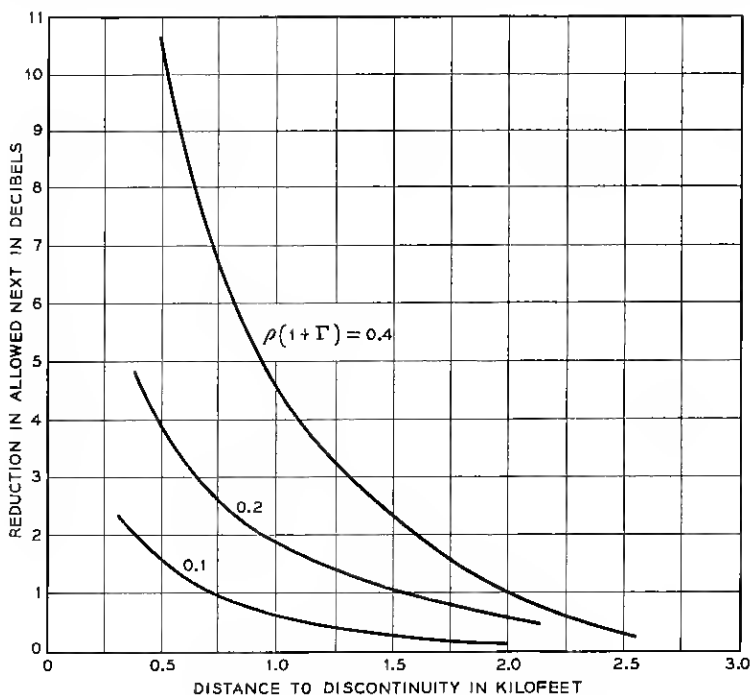


Fig. 35 — Effect of reflected signals on NEXT performance.

levels, and/or increasing preamplifier gain. Up to 6 db of padding is possible by a combination of these means without materially affecting the repeater design. It does not appear that further action is required, though a "bad environment" regenerator has been considered. A possible implementation is shown in Fig. 36; the feedback windings have been placed on a separate core.

7.1 Requirements

The following requirements have been set for the regenerator:

Height of output pulse	$3v \pm 0.3$ volt
Unbalance in height of positive and negative pulse	± 0.15 volt
Width of output pulse (half amplitude)	0.32 ± 0.03 μ sec
Unbalance in width of positive and negative pulse	± 0.015 μ sec
Maximum rise or fall time	0.090 μ sec

The variation in the height of the output pulse is primarily controlled by the variation in supply voltage. The 6-volt supply of Fig. 34 is derived from a zener diode, ± 10 per cent voltage control being quite economical. The effect of the transistor "on" voltage is extremely small,

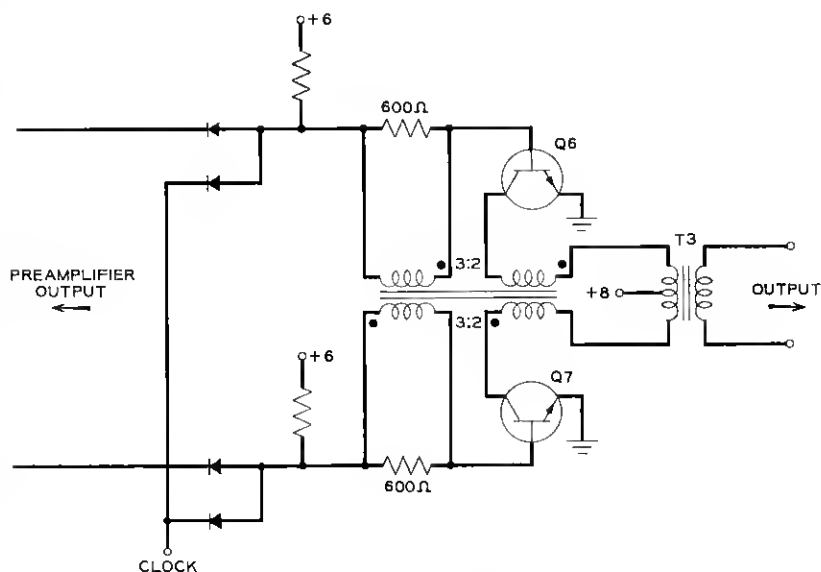


Fig. 36 — Modified regenerator.

$V_{\text{CE SAT}}$ being typically 0.3 volt for the transistor used for the operating conditions designed. The allowed unbalance requirement is primarily a transformer balance requirement. The effect of $\Delta V_{\text{CE SAT}}$ is slight, typically about 0.1 volt (compared to 6-volt supply).

The width of the output is controlled by the clock and transistor rise and fall times and the response of the output transformer. The transistor requirements derived allow a rise time of $0.06 \pm 0.01 \mu\text{sec}$ and a fall time of $0.035 \pm 0.015 \mu\text{sec}$. For the diffused silicon transistors used, the turn-on time requirements set the gate current at 2 ma, giving a switching current gain of 7.5. The requirement on pulse width control greatly dominates any criterion for regeneration.

7.2 Feedback Ratio

The feedback voltage is bounded in magnitude by reverse emitter breakdown in the regenerator transistors on the one hand and by noise margin on the other. The peak negative signal delivered by the preamplifier to the gate is approximately $3/2 E_m$. The maximum reverse voltage seen by the base-emitter junction of the blocking oscillator transistor is

$$V_{\text{BER}} = 3/2 E_m + V_f - V_d \quad (89)$$

where V_f is the feedback voltage and V_d is the gate diode forward drop, typically 0.7 volt. The curves labelled "max" in Fig. 37 show the allowed V_f as a function of peak received pulse amplitude for various values of $V_{\text{BER max}}$. For $V_{\text{BER}} = 7$ volts (minimum for the transistors used), and $E_m = 3$ volts, V_f must be less than 3.2 volts.

When one half of the regenerator is operating, its gate point falls V_f volts. Should the signal fall more than V_f volts below threshold, it may turn off the regenerator prematurely. The voltage at the preamplifier output is approximately

$$v = e_s + n(t) - \frac{E_m}{2} \quad (90)$$

where e_s is the received signal and may be represented by (worst case)

$$e_s = E_m \sin \omega_0 t \quad (91)$$

$$v = E_m (\sin \omega_0 t - \frac{1}{2}) + n(t). \quad (92)$$

If regenerator turn-on is initiated at the peak of the received pulse, the greatest change that can occur in the received signal (less noise) while

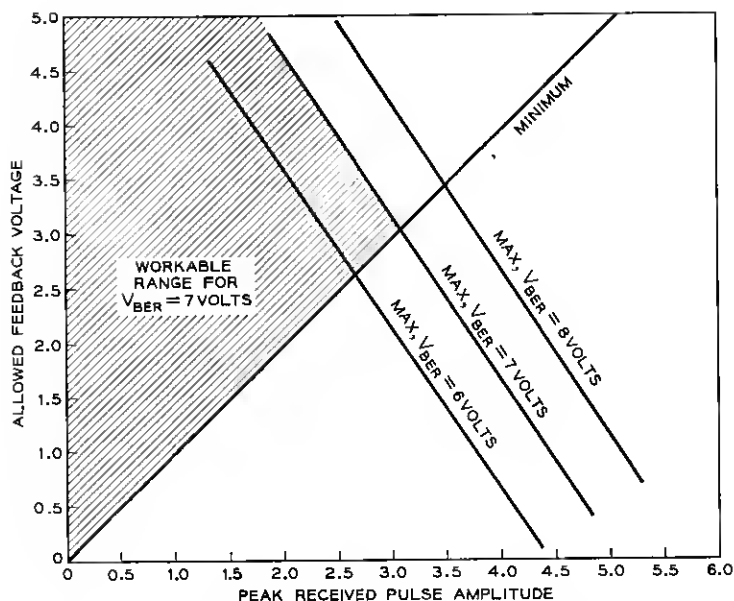


Fig. 37 — Maximum and minimum allowed feedback voltage.

the regenerator is on is $E_m/2$, so the most negative the gate can go during regeneration is

$$v_{\max} = \frac{E_m}{2} + n(t)_{\max}. \quad (93)$$

The $n(t)_{\max}$ cannot exceed $E_m/2$ in a workable repeater so

$$v_{\max} \leq E_m. \quad (94)$$

It is then safe to feed back a voltage as small as E_m , as shown by the curve labelled "minimum" in Fig. 37. Thus, for $E_m = 3$ volts, V_f must be ≥ 3 volts to ensure uninterrupted regeneration and V_f must be ≤ 3.2 volts to prevent reverse emitter breakdown. The feedback voltage is thus set equal to the regenerator output level (3 volts), making the primary-to-output-to-feedback windings ratio for T_3 equal to $4CT:1CT:1$.

Leakage inductance in T_3 affects the turn-on of the regenerator, particularly the "maybe" region of regeneration. If the received signal exceeds threshold by Δ volts at the sampling instant, this voltage is im-

pressed across the feedback winding and must produce sufficient current in the base of Q_6 or Q_7 to turn these units on within the width of the time crosshair, or perhaps more importantly, must not greatly affect the output rise time. It appears quite sufficient if a $\Delta = 0.1$ volt allows the base current to build up to 0.5 ma in $0.01 \mu\text{sec}$, or the leakage inductance of T_3 is less than $2 \mu\text{henrys}$ looking into the feedback winding. If the high-frequency cutoff of T_3 is due to leakage inductance, this cutoff must then exceed 7 mc.

Capacitance of the feedback windings-to-ground affect the delay and rise time of the regenerator. With the clock output returned to -1.5 volts and 2 ma gate current, the delay due to gate capacitance is $0.7 C$ nanoseconds with C in μmf . Capacitances up to $20 \mu\text{mf}$ can be tolerated provided the two gates are approximately balanced. Because the transformer used has unbalanced feedback winding capacitances (approximately 15 and $25 \mu\text{mf}$), the gate currents have been made to differ slightly to produce the same pulse widths for both the positive and negative pulse output. Perhaps a better arrangement, at the expense of a component, is to build out the capacity of the low-capacity winding.

It is worth noting that the regenerator may be triggered into self-oscillation in the absence of a received signal (clock). This cannot be prevented so long as the same gate diode is used for spike sampling and turn-off. Actually, the amount of received clock required to dampen the self-oscillation is so small that the clock energy received via near-end crosstalk is generally sufficient to dampen the oscillation. The oscillation, when it occurs, is not detrimental to the repeater circuit.

The RL network shunted across the repeater output as a nonlinear equalizer (Fig. 19) has two important effects on the regenerator that will be treated only superficially. First, the afterkick of the network is coupled into the regenerator feedback windings. This has the effect of reducing intersymbol interference or, equivalently, of partially invoking the bipolar rule at each repeater. The feedback voltage is made equal to a few tenths of a volt at the next sample instant to discourage, to the extent desired, the output of successive pulses of common polarity.

A second effect of the network is that the afterkick coupled into the feedback winding affects the rise time of the output. The net effect is that when an output pulse is immediately preceded by a pulse (which must be of opposite polarity), it rises sooner than would be the case otherwise; this additional area on the front of the pulse aids in cancelling the tail of its predecessor, thereby further reducing intersymbol interference. Because the faster rise time is pulse-correlated, its effect on the position of the received pulse peak is straightforward, and properly

applied, the technique can even improve the pattern jitter performance of a repeater.

VIII. SECONDARY FEATURES

8.1 Power Arrangement

Repeaters are to be powered over the signal pair. Of all the series and shunt power arrangements, the simplex current loop of Fig. 38 is the most attractive. A constant current is fed over the phantom of the EW and WE circuits, and the voltage at each repeater is obtained across a zener reference diode.

For 22-gauge cable, the maximum line resistance (140°F) in the current path is approximately 116 ohms for 6000-ft span length. Optimum power transfer to the repeater circuit then occurs when the current demanded by the repeater, I_0 , and the operating voltage for the repeater, E_0 , satisfy

$$E_0 = 116 I_0. \quad (95)$$

Diffused-base transistors are noted for their alpha defect at low current, and an average current of about 5 ma/stage is required to maintain reasonable gain. This accounts for 35 ma per one-way repeater. Power considerations make it not always possible to design for minimum current, and considering base drives and other current demands, minimum current drain per one-way repeater for the signal levels desired and the transistors used is approximately 50 ma.

For reasons of economy, as well as ability to power maximum-length spans, it is convenient to design one power unit for a two-way repeater

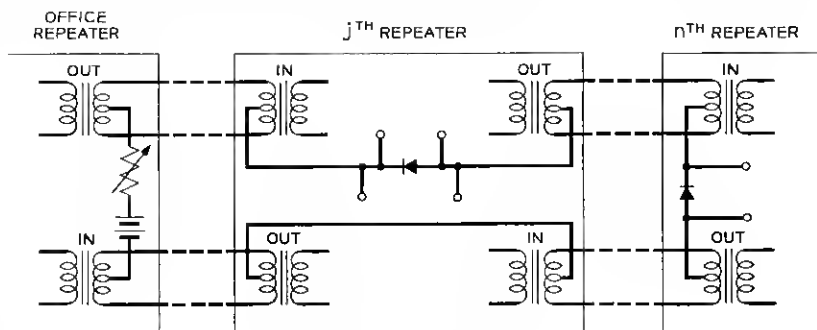


Fig. 38 — Simplex power loop.

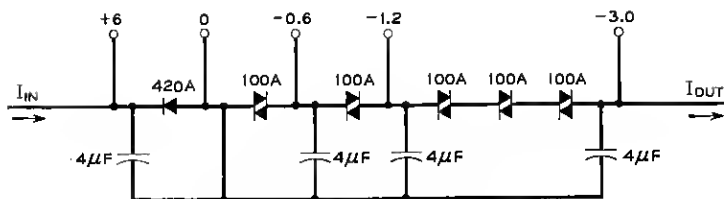
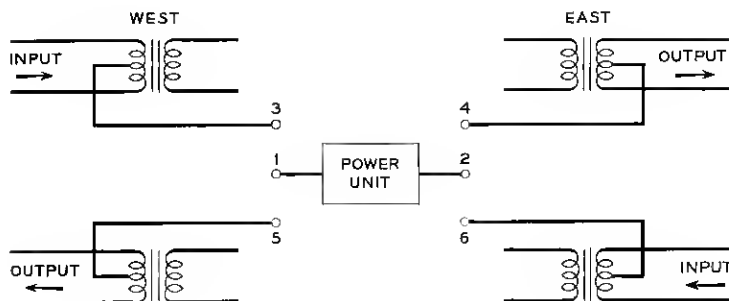


Fig. 39 - Twin repeater power unit.

(twin repeater circuits in one enclosure). The repeater designed is such a "twin" unit with common power supply. It operates with a minimum current of 110 ma and has a voltage drop of 9 volts (which is almost optimum for nominal temperature). This voltage is derived from a 6-volt zener diode and several click-reducer diodes as shown in Fig. 39. The voltage required for the power loop is then 22 volts per section. Using a +130 and -130 volts in the office, 11 sections may be powered, corresponding to 12.5 miles per office or 25 miles maximum interoffice spacing.

The power options on the repeater are shown in Fig. 40. Power may be routed through the repeater in either direction. It may be looped back readily, and under the loopback condition, the repeater at the loopback point may be powered from either end of the line. The option requires 6 terminals. By eliminating some of the minor options, the number of terminals may be reduced.



1. STRAIGHT THROUGH _____ 1 TO 3, 2 TO 4, 5 TO 6
2. LOOPBACK, POWER FROM EAST _____ 1 TO 6, 2 TO 4, 3 TO 5
3. LOOPBACK, POWER FROM WEST _____ 1 TO 3, 2 TO 5, 4 TO 6

Fig. 40 — Repeater power options.

The two halves of the "twin" repeater, with midspan power loopback, serve 24 two-way voice channels or 48 one-way channels.

8.2 Protection

The transistors used are low-power devices, and any transistor circuit attached to exposed cable must consider the problem of lightning surge activity.

P. A. Gresh and D. W. Bodle of Bell Laboratories have divided the plant into three exposure classes: (1) low exposure typified by underground plant, (2) moderate exposure typified by aerial and buried cable in suburban and rural areas, and (3) high exposure typified by unshielded

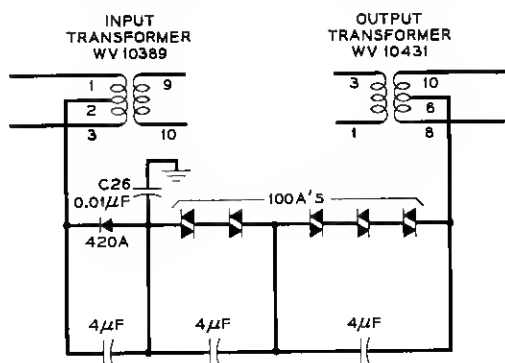


Fig. 41 — Repeater power circuit.

facilities such as open wire or distribution wire. Only the first two classes will be considered as potential PCM environments.

8.2.1 Repeater Capability

Repeaters may be subjected to either longitudinal or metallic voltage or current surges. Longitudinal surge currents flow through the power circuit (Fig. 41), producing currents at the secondary of the input transformer and the primary of the output transformer diminished by 40 db (the balance requirement placed on the transformers). The primary effect of longitudinal surge current is in the power zener. The unit used, WE420A, has a reverse surge current capability of the order of 10 amperes.*

* All surge currents will assume a near triangular wave of 10 μ s rise and 600 μ s fall times.

Longitudinal voltages are impressed across the by-pass capacitor C_{26} , and across the entire repeater circuit to ground. The circuit to can and C_{26} breakdown voltage must exceed expected surges, and has been set at 1000 volts. Longitudinal voltages may exist, particularly at power loopback points, between the repeater input and output terminals and the repeater circuit. There, transformer windings must be insulated against surge voltages, a difficult situation with small pulse transformers. However, 1000 volts surge breakdown has been achieved in the transformers used.

Metallic currents induce sizeable currents into the transistor circuits. These currents cannot readily damage the input transistors Q_1 and Q_2 because of the large emitter and collector resistors associated with these stages. The output transistors Q_6 and Q_7 are not so protected. Tests indicate these transistors will fail for metallic line surges of 5 to 10 amperes. Further protection is available by limiting the metallic voltage by shunting the line with semiconductor diodes, such as the 100A click-reducer diode, which is capable of surge currents up to 80 amperes. Six or more units must be used to prevent clipping of the repeater output signal. These diodes also protect the transformer windings which, however, have been found in limited tests to be able to withstand surges of 50-100 amperes.

8.2.2 Class 1 Repeaters

Gresh and Bodle found very slight lightning activity in their Class 1 environment. The 1000-volt longitudinal voltage capability and the 10-ampere longitudinal and 5-ampere metallic surge current capability should be sufficient for this class, except for repeaters mounted in central offices with carbon block line protection. Breakdown of the carbon block will convert longitudinal surges to metallic surges and may damage the output transistors. For this reason it is felt that with carbon blocks on a PCM line, the repeater output should be shunted by the 100A click-reducer diode string. At the office, the power unit of the repeater is generally returned through a current-limiting resistance to a power source. This resistance should not be less than 10 ohms so that carbon block breakdown does not damage the zener diode.

Then, for Class 1 exposure, line repeaters have no special protection. Office repeater outputs have 100A diode protection.

8.2.3 Class 2 Repeaters

For Class 2 exposure, the 1000-volt insulation and 10-ampere longitudinal current capability are inadequate. There are two major alterna-

tives: (1) better insulated input and output transformers and a heavy-duty zener diode, or (2) carbon block or gas tube protection for each repeater. The problem is still under study. The interim solution uses carbon block and 100A diode protection on both the input and output of each Class 2 repeater, and builds out the power supply impedance with a small resistance (10–20 ohms) to limit the surge current. A better solution would likely require a high-power zener diode, and gas tube protection for the transformers, all built within the repeater can.

8.3 Maintenance Equipment

8.3.1 Error Meter

One acid test of the performance of a repeated line is a test of line error rate. Indeed, if the basic design assures adequate phase jitter performance, the error rate test is all important.

With pseudo-ternary transmission according to some basic law, such as bipolar, measurement of error rate is very simply accomplished by observing the number of pulses per unit time that violate the basic code. For bipolar transmission one looks for those pulses that fail to obey the alternate polarity rule. A circuit to accomplish this is shown in Fig. 42. Its operation is straightforward and will not be discussed. Suffice it to

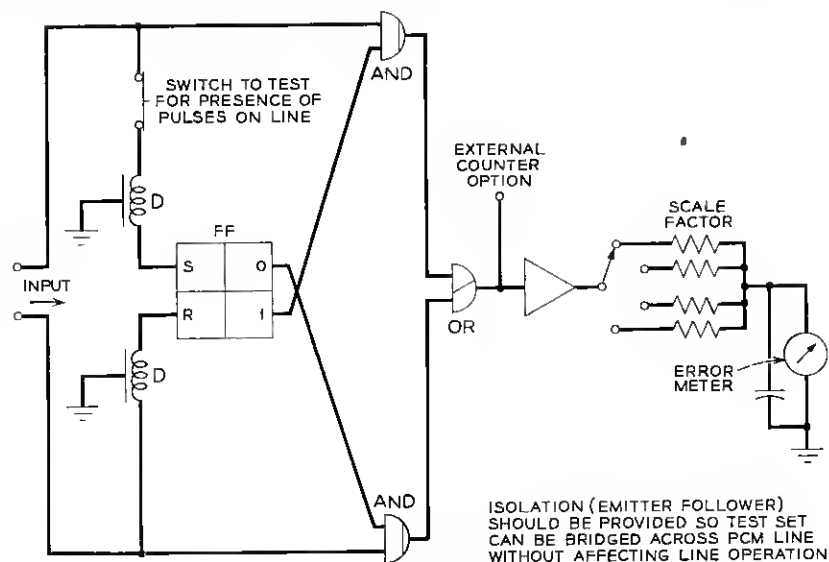


Fig. 42 — Proposed error rate meter for exchange carrier PCM.

say the circuit detects all single errors and most multiple errors. A comparison of bipolar violations per second against actual errors per second for various error rates has been established empirically and is shown in Fig. 43. There are, of course, certain types of errors that could conceivably occur in large numbers that would not be detected by the error meter.

The meter may be placed across an operating line to evaluate the performance of the line without affecting the operation of the line. Conceptually, it is as simple to use as a simple voltmeter.

8.3.2 Marginal Checking

The contemplated PCM system operates with large numbers of tandem repeaters. Provision for remote identification of a faulty repeater is a requisite, particularly in the exchange cable environment characterized by severe NEXT. Lacking a complete description of NEXT (particularly the tail of the distribution), it seems likely that an aging repeater will make excessive transmission errors before failing altogether. Indeed, a PCM route may work satisfactorily for years, then

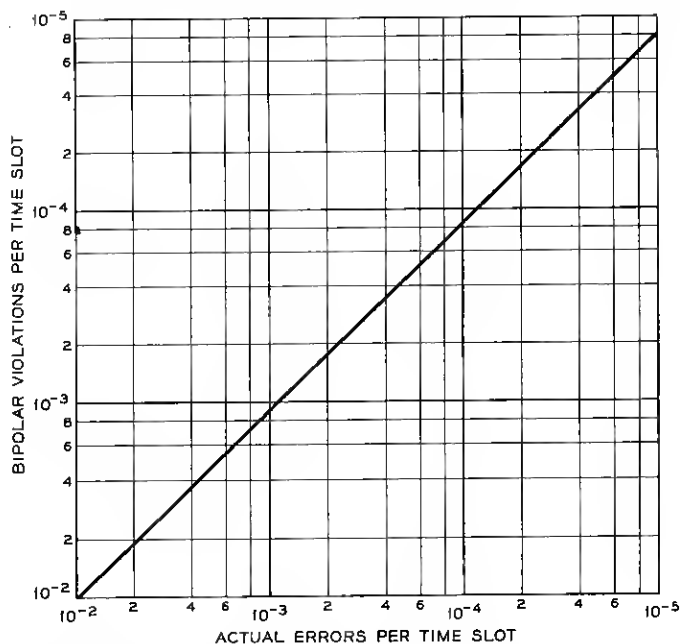


Fig. 43 — Comparison of error rates, actual and as indicated by error meter, for errors generated by exposing working repeater to random noise.

fail due, perhaps, to increased density of PCM in the cable. Remote marginal checking, as well as fault location, seems extremely desirable.

What meaningful parameter may be varied from a central office to produce failure of a line? The author has concluded that in view of the pulse-detection process, the most meaningful parameter available for remote testing is the balance of the transmitted bipolar pattern. This parameter gets to the very heart of the repeater — the decision-making — for the greater the unbalance in the pulse train, the smaller the opening of the eye. The marginal check parameter is then the number of unipolar pulses that may be superimposed on a bipolar wave before a repeater malfunctions.

Perhaps the simplest method for identification of one of many serially operated units associates an identification tone with each equipment location. It is then convenient to associate a particular marginal check frequency and filter with each manhole along a repeater route. The filter may serve many repeaters and is coupled to the outputs of the many repeaters at a common location. A special test PCM pattern may be transmitted to excite any selected repeater along a route. The output of the filter is returned to the office over a marginal checking cable pair. The general plan is shown in Fig. 44.

If the identification frequencies are in the audio band, a balanced bi-

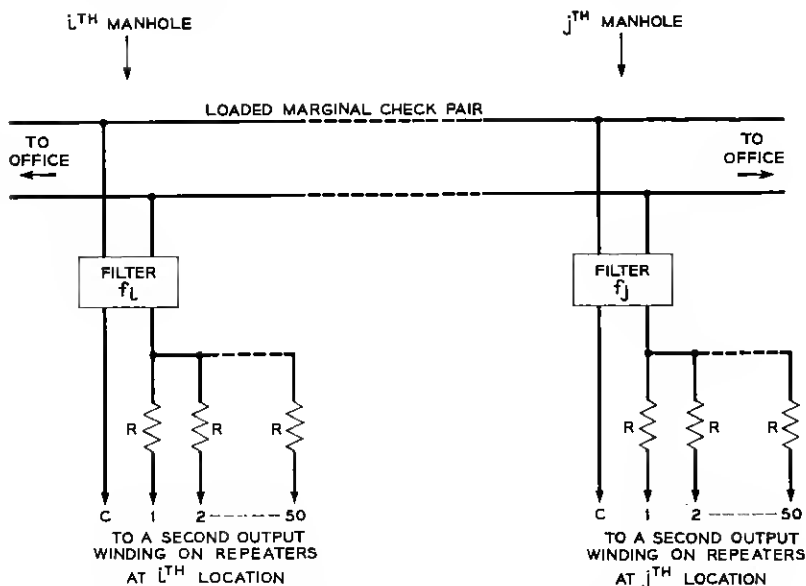


Fig. 44 — General plan for marginal checking 25 two-way systems.

polar pulse train contributes very little energy to the filter output. On the other hand, added unipolar pulses gated on-off at an identification frequency provide considerable excitation to the filter. Furthermore, the return signal should be proportional to the unipolar density up to the point of repeater failure. The margin of operation of a repeater is then given by the number of unipolar pulses that may be added to a bipolar train before the return signal fails to be proportional to unipolar density. In practice, a sparse unipolar density is transmitted and the return signal amplitude adjusted to a reference mark on a meter. As the unipolar density is increased, the meter must go to calibrated markings. When the meter fails to toe the mark, the unipolar density is a measure of the margin in the repeater under test or any repeater that precedes it. The indication that the meter gives under the marginal condition is an indication of the type of failure.

How many repeaters may a single filter serve? A random bipolar signal with probability of a pulse being present equal to 0.5 has a power density spectrum

$$W(\omega) = \frac{1}{16\pi^2} (1 - \cos \omega) \left(\frac{\sin \omega/4}{\omega/4} \right)^2 \quad (96)$$

where frequency has been normalized to the bit rate, and the signal is assumed to be one volt peak amplitude applied to a one-ohm load.

If $\omega \ll 1$

$$W(\omega) \approx \frac{\omega^2}{32\pi^2}. \quad (97)$$

The power resulting from passing N such signals through a band-pass filter of bandwidth Δf is

$$P_N = \frac{\omega^2 N}{16\pi} \Delta f. \quad (98)$$

A unipolar signal of pulse density d burst on-off at frequency ω_1 produces a signal of amplitude d/π , or power

$$P_s = \frac{d^2}{\pi^2}. \quad (99)$$

Thus, the signal returned consists of P_N due to the disturbance of N operating systems and P_s due to the desired return signal

$$\frac{P_s}{P_N} = \frac{16d^2}{\pi N \omega^2 \Delta f}. \quad (100)$$

Even for a 20-db signal-to-noise ratio, a sparse unipolar pattern ($d = 1/32$), with a fault-location frequency of 3 kc and a $2\pi\Delta f = 0.01\omega$ (typical conditions), N is extremely large. Consequently, when working in the audio range, one filter may readily serve 50 repeaters from an interference point of view. Equipment boxes will be designed for 25 two-way repeaters, and for various reasons it is felt that there should be one marginal checking pair per repeater box.

Perhaps the greatest problem in this area lies in absolute signal levels. If there is no power gain in the marginal check filter and 50 repeaters are resistively coupled to that filter, and if the output of the filter is transmitted up to 12.5 miles back to an office, the received power level is exceedingly small. Typical major losses are given in Table V.

To keep line transmission loss down to 0.9 db/mile, audio frequencies and loaded cable have been employed. The signal available at the repeater output is about -27 dbm for $d = \frac{1}{32}$.

The situation is summarized in Fig. 45. For example, for $d = \frac{1}{16}$, transmission over 12.5 miles of loaded cable (requiring measurement from each end of a 25-mile system) produces a signal level at the office of -77 dbm. For $N = -70$ dbm (thought to be near worst-case office noise level across the 1.5 to 3-kc band if certain harmonics of 60 cps are avoided), the receiver bandwidth must be less than 75 cycles for a 6 db S/N ratio. Or a signal with $d = \frac{1}{32}$ over 12.5 miles requires a receiver bandwidth of about 20 cycles for a 6-db S/N ratio. The situation is somewhat different if peak detection is used (20 log bandwidth ratio applies).

It is felt that reasonable unipolar densities are $d = \frac{1}{32}, \frac{2}{32}, \frac{3}{32}, \frac{4}{32}$. The repeater will be only slightly affected by $d = \frac{1}{32}$, but will almost surely fail for $d = \frac{4}{32}$. The effect of the added unipolar pattern in reducing operating margin is shown in Fig. 46. The difference in performance for positive or negative added pulses results from the action of the half-wave rectifier that controls the automatic threshold circuit.

With $d = \frac{1}{32}$, there is a quantized set of tones available as fault-loc-

TABLE V — MAJOR SIGNAL LOSSES

Repeater Output Transformer (1.5 kc).....	16.0 db
Filter Matching Loss.....	4.0 db
Filter Transmission Loss.....	3.0 db
Coupling Loss.....	16.5 db
Other Losses.....	5.5 db
	<hr/> 45.0 db

Line Transmission Loss 0.9 db/mi.

tion frequencies, corresponding to the number of unipolar pulses allowed per burst. There are 17 such frequencies in the band 1.005 to 3.017 kc. Such close-spaced frequencies put rather stringent requirements on the marginal check filter. The filter should offer 20-db rejection of adjacent frequency tones, provide maximum power transfer to the loaded pair, not load the audio pair at frequencies out of its passband, and have a pass-band, preferably, that is independent of the distance from the line-driving point to the nearest load coil. Suffice it to say that such a filter has been designed.

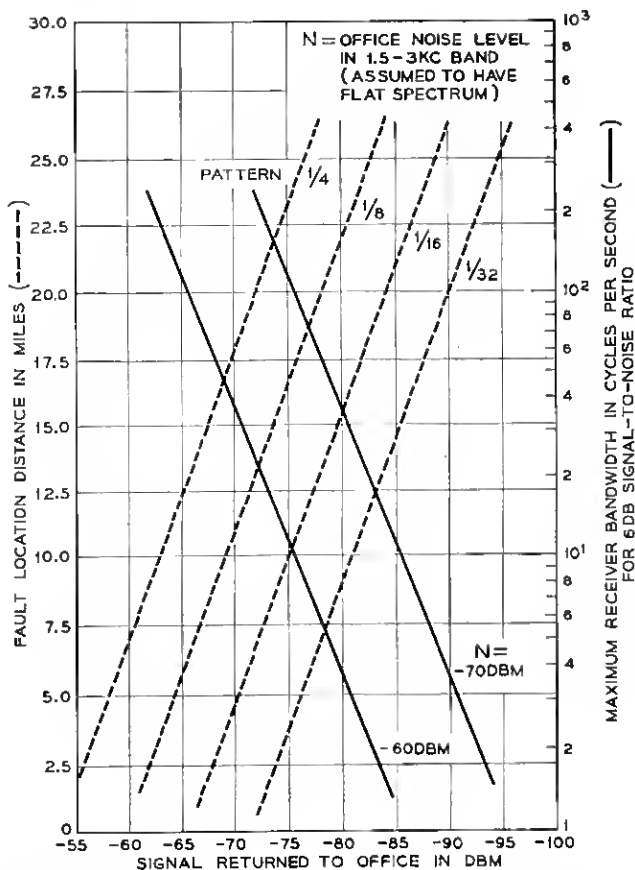


Fig. 45 — Received signal for various distances and patterns, and required receiver bandwidth for various received levels and office noise.

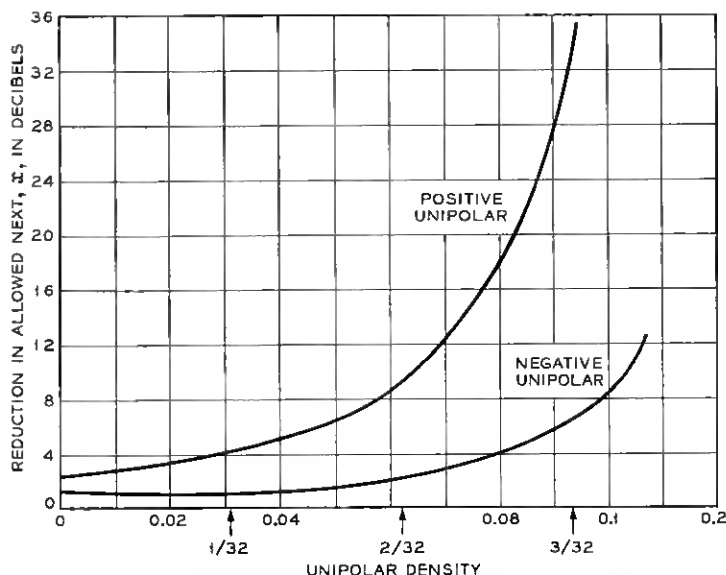


Fig. 46 — Effect of added unipolar pulses on NEXT performance.

8.4 Equipment Design

The guide words for the equipment design are size and reliability. Size is of utmost importance, for a repeater is expected to be manhole mounted, and manhole space is quite valuable. Manhole enlargement is generally sufficiently expensive that, if required, it represents a sizeable fraction of repeater cost, even when divided up among many repeaters. On the other hand, a manhole repeater must be extremely reliable. It would be a mistake to sacrifice reliability for size, for example, for the feasibility of operation of the proposed system demands a very high degree of reliability. For example, a 25-mile repeatered line will contain about 350 transistors, 675 diodes, and 2350 other components. With a reliability figure of 0.1 per cent per 1000 hours for transistors, the line could be expected to fail every 3000 hours (125 days) from this cause alone. At 0.01 per cent per 1000 hours, the line should fail every 1250 days (3.4 years). A complement of 25 repeatered lines along a 25-mile route would develop trouble every 5 days for the 0.1 per cent figure and every 50 days for the 0.01 per cent figure. It is expected that routes will be sectionalized and spare lines incorporated into the system.

So, miniaturization should not be achieved at a sacrifice to reliability.

For this reason, standard, well-known components are used throughout. Only the timing inductor represents a special component development. Diminutive size is achieved by a three-dimensional packaging of the components.

The three-dimensionality is achieved by assembling sub-blocks of the circuit into small component modules, as shown in Fig. 47. These modules are assembled (as if they were components) onto a master board as shown in Fig. 48. The 135 components are packaged into a can of overall dimensions $5\frac{3}{4} \times 3\frac{1}{8} \times 1\frac{1}{16}$ inches.

There are three options on the two-way assembly. As shown in Fig. 49, the center screw terminal is a power option that controls the power flow through the repeater. An LBO option for each half of the repeater is located on the corners of the master board. The LBO network is a single connection for nominal cable length. For other lengths, a network secured by the three screws replaces the simple strap shown. The three screws make the required connections from LBO to printed wiring board.

Fig. 50 shows the printed wiring side of the repeater. Inputs, outputs, ground, and the marginal checking output appear on the printed wiring connector.

Thirty repeaters have been built in the manner of Figs. 48–50.

8.5 Terminal Repeaters

In addition to the normal line repeaters, special repeaters are required at the transmitting and receiving terminals.

The transmitting repeater utilizes the terminal clock. It has no cross-talk problem, and is peculiar only in that it must convert the unipolar



Fig. 47 — Small component module.

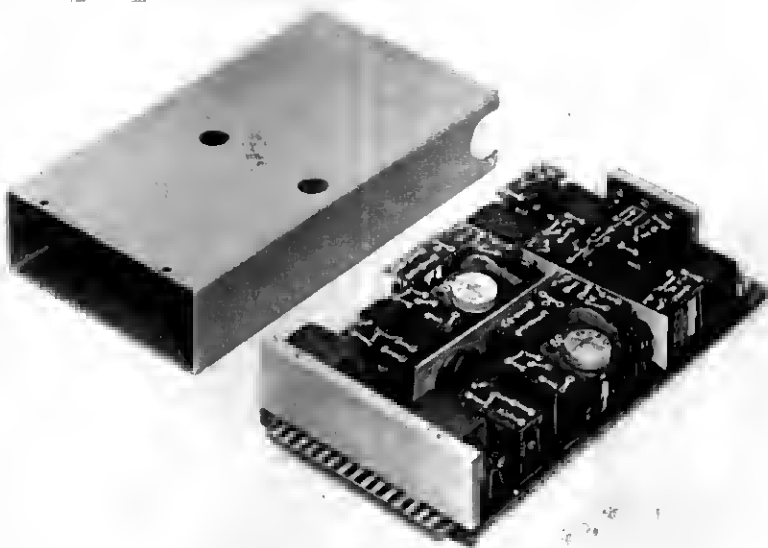


Fig. 48 — Experimental PCM repeater, cover removed.



Fig. 49 — Another view of repeater circuit.

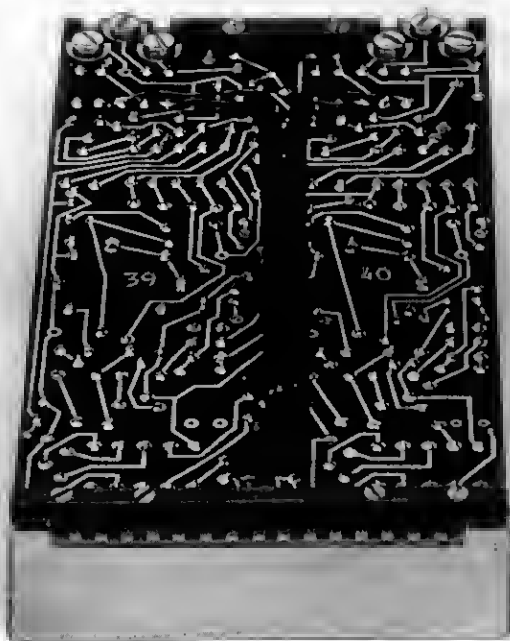


Fig. 50 — Printed wiring of repeater.

terminal signals to a bipolar pattern. This is done by use of a regular repeater regenerator with flip-flop control of the input gates to enforce the alternate polarity rule. The flip-flop is set and reset by the regenerator output. A block diagram is shown in Fig. 51.

The receiving repeater must deliver a unipolar signal and clock to the receiving terminal. The design is very close to a regular repeater with the bipolar regenerator replaced by an OR gate and unipolar regenerator. The output of the repeater clock circuit is used to drive a clock amplifier that provides a square wave of clock, properly positioned, for the receiving terminal. Fig. 52 shows a block diagram. In many ways a regular repeater circuit at the receiving terminal is desirable. In particular, in the design of Fig. 52, the error meter cannot be readily used at the receiving terminal.

These repeaters are physically a part of the experimental terminal, and the equipment design is consistent with the over-all terminal design.

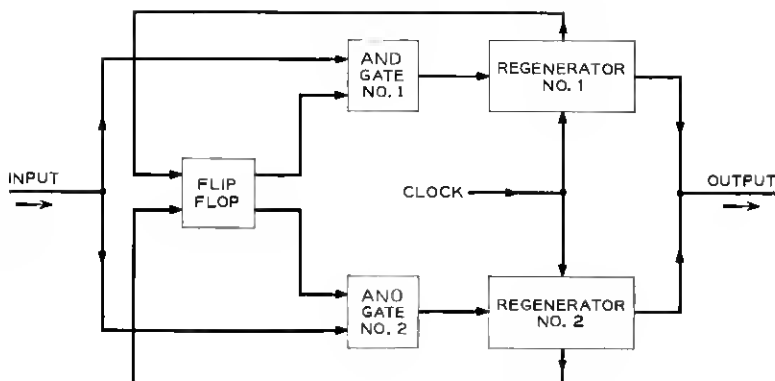


Fig. 51 — Block diagram of transmitting repeater.

IX. PERFORMANCE EVALUATION

Two parameters dominate the performance evaluation picture. First the repeater must maintain acceptable crosstalk performance over life and temperature. Secondly, the jitter due to random pattern changes and any other phenomena on the output pulse must be sufficiently controlled that a 25-mile system will deliver an acceptably stable signal to the receiving terminal. But first consider the simple operation of the repeater.

9.1 Operating Waveforms

Fig. 53(a) shows the repeater output signal which is applied to the transmission medium. The particular pattern displayed consists of three

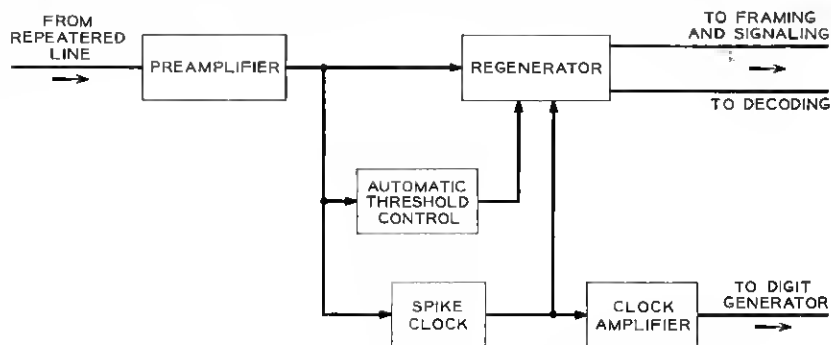


Fig. 52 — Block diagram of receiving repeater.

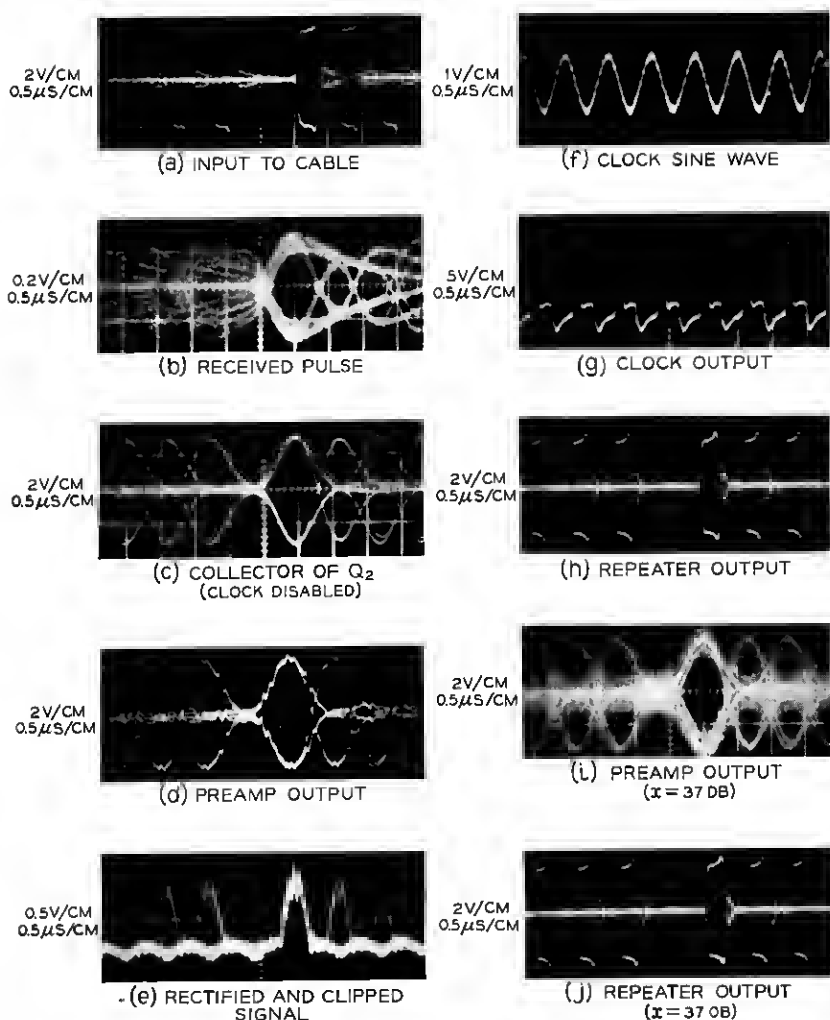


Fig. 53 — Operating waveforms. One large division in the illustration equals one cm.

random pulses followed by a forced space, followed by a forced pulse, followed by 3 random pulses. The pulses are 3 volts in amplitude.

Fig. 53(b) shows the signal after transmission through 6300 feet of cable as it appears at the secondary of the input transformer. The peak pulse height is about 0.25 volt, and a pulse is spread out over about 4 time slots.

Fig. 53(c) shows the amplified and equalized train as it appears on

the collector of the output stage of the preamplifier. The pulses are now about 3 volts in amplitude and essentially resolved to a single time slot. For this picture the repeater clock has been disabled.

Fig. 53(d) shows the signal at the secondary of the preamplifier output transformer. The signal has been shifted by the automatic threshold circuit to achieve the threshold and clock clipping function. The waveform has pronounced "nicks" that are a result of periodic gate current flow in the leakage inductance of the transformer.

Fig. 53(e) shows the rectified and clipped signal ready for delivery to the clock circuit.

Fig. 53(f) shows the sine wave at the tap point of the timing inductor.

Fig. 53(g) shows the clock output at the secondary of the clock output transformer. The positive-going spike samples the incoming wave; the negative-going spike shuts off the regenerator.

Fig. 53(h) shows the repeater output wave which is again applied to the transmission line.

Fig. 53(i) is the same as 53(d) with a crosstalk signal introduced through 37 db of loss ($x = 37$ db).

Fig. 53(j) is the output signal corresponding to Fig. 53(i). The output error rate is set to one error per 10^5 time slots.

9.2 Crosstalk Performance

Although work has been done with actual cable, it was convenient, for the most part, to use a simulated crosstalk path. An experimental crosstalk set-up is shown in Fig. 54. A small coupling capacitor is used to produce a crosstalk path-frequency characteristic that slopes at 6 db per octave in the frequency range of interest. For this set-up 1.544-mc

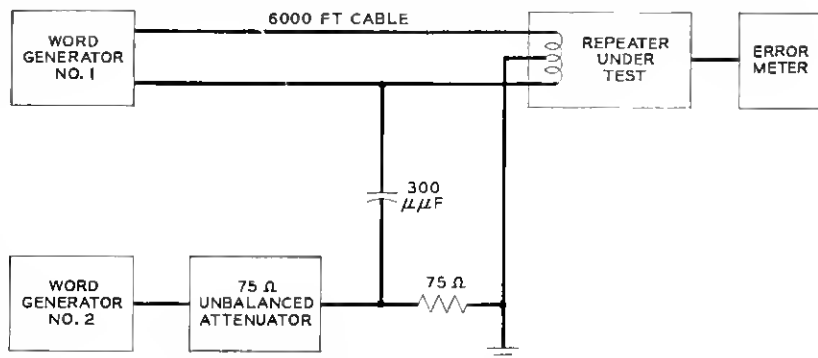


Fig. 54 — Experimental crosstalk simulator.

crosstalk coupling loss (x) is obtained by adding 24 db to the attenuator setting.

9.2.1 Information Path

Over-all crosstalk effect on repeater performance has been measured in terms of the allowed x versus the time and voltage crosshair positions, both varied forcibly without affecting other repeater conditions.

Typical effect of time crosshair position is shown in Fig. 55. This experimental curve should be compared to Fig. 30. The experimental clock sample width is $0.1 \mu\text{sec}$. With perfect voltage crosshair positioning and performance, Fig. 30 predicts $x = 33 \text{ db}$ for $\epsilon = 0$; the measured value is 35 db. A shift of 30° ($\epsilon = 30^\circ$) reduces the allowed crosstalk by 1.3 db ideally (Fig. 30). The measured value is 1.3 db for a 30° lead and slightly less than 2 db for a 30° phase lag. One concludes the allowed instability in repeater clock phase should not penalize crosstalk performance (x) by more than 1 to 2 db.

For similar conditions, the clock was unaltered and the threshold voltage varied. For each voltage crosshair position, the value of x that produces 10^{-6} error rate was recorded. The result is shown in Fig. 56. From Fig. 24, for a 2 db reduction in allowed NEXT, $\Delta = 0.10h_x$, and from

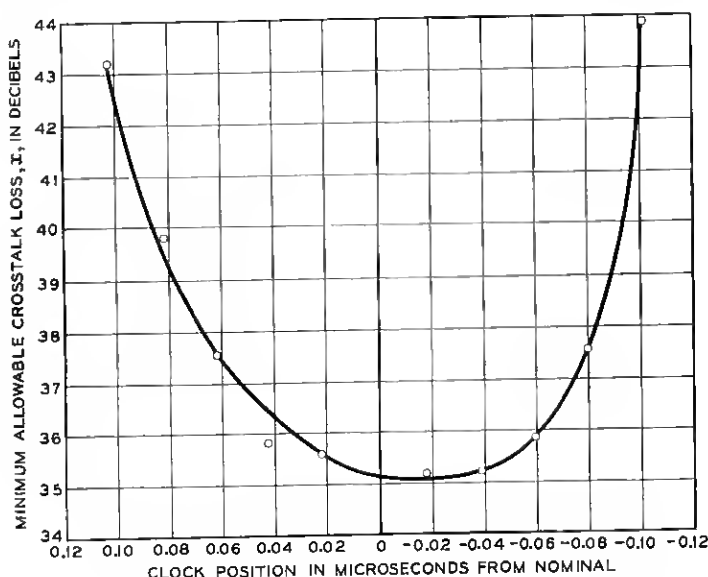


Fig. 55 — Typical measured effect of clock phase on crosstalk performance.

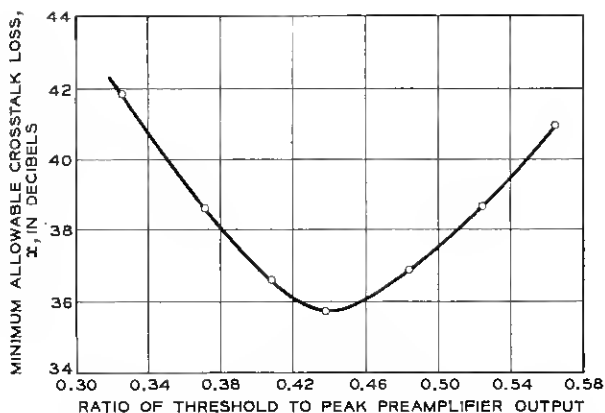


Fig. 56 — Typical measured effect of threshold on crosstalk performance.

Fig. 56, $\Delta = 0.06E_m$, suggesting $h_x = 0.6E_m$. It appears that only 60 per cent of the peak received pulse height exists as the eye height at the extreme of the jittered time crosshair position.* Fig. 29(a) predicts 30° of clock jitter for $x = 35$ db and Fig. 30 predicts a 1.3 db crosstalk penalty for the 30° shift, suggesting that the peak height of the eye is approximately 70 per cent of the received peak pulse height. Thirty per cent of the potential eye is thus lost to intersymbol interference, undershoot, bipolarity unbalance, noise pickup in the test cable, and deviation of reality from the analytical assumptions. Examination of Fig. 53(c) and 53(d) leads one to expect this result.

9.2.2 Timing Path

The simulated crosstalk path was used to examine the timing crosstalk performance. In this case, for various transmitted and received patterns, crosstalk loss was adjusted to produce $\pm 30^\circ$ maximum clock jitter. These values of x are recorded in Fig. 57. They are averaged, first by column, then completely. For each transmitted pattern, an "equivalent" timing frequency is recorded. This is the frequency where the cable loss is 5 db less than the crosstalk loss, and does not depart greatly from 772 kc. In some cases, the equivalent frequency falls below 772 kc, particularly due to dense transmitted pattern-sparse interfering pattern. It should be noted that odd patterns (odd numbers of pulses per word) produce harmonics of 96.5 kc, while even patterns produce harmonics of

* Bear in mind that changing the threshold voltage affects clock clipping and therefore alters the phase of the clock.

		TRANSMITTED PATTERN									
		1/8	2/8	3/8	4/8	5/8	6/8	7/8	8/8	1/4	1/2
CROSSTALK PATTERN	1/8	42	27	32	<24	26	<24	<24	<24	27	<24
	2/8	34	39	27	34	<24	30	<24	27	39	34
	3/8	44	32	39	29	34	26	32	25	32	28
	4/8	36	42	31	39	29	35	27	27	40	30
	5/8	44	33	40	32	39	29	35	29	35	31
	6/8	38	41	33	39	31	38	30	29	40	35
	7/8	44	33	40	32	39	31	38	30	35	33
	8/8	35	41	33	39	32	39	31	37	35	34
	1/4	32	36	25	33	<24	26	<24	30	42	25
	1/2	33	38	29	29	26	29	25	24	31	42
	AVG	38	36	34	33	31	31	29	28	35	31
	f _e	900	820	760	740	660	660	630	600	800	880
GRAND AVG											33
											740

LINE LOSS = 32DB AT 772 KC, 48 DB AT 1.5 MC

f_e = EQUIVALENT TIMING FREQUENCY (WHERE LINE LOSS IS 5 DB LESS THAN CROSSTALK LOSS BASED ON ABOVE 1.5 MC FIGURES) IN KC.

n/8 MEANS AN 8-DIGIT WORD OF n SUCCESSIVE PULSES.

1/n MEANS ONE PULSE EVERY n TIME SLOTS.

Fig. 57 — Values of x that produce 30° of timing jitter.

193 kc. The result is that worst interference exists when both patterns are either odd or even.

9.3 Pattern Shift

R. C. Chapman of the Laboratories has studied the mechanism and result of phase jitter accumulation along a string of PCM repeaters. The result of his work (based on a simple model), which also considers the nature of the PCM terminals, indicates satisfactory terminal performance should result from PCM line lengths up to 25 miles if the repeater clock circuit Q is greater than 50, and the worst-case variation of delay

(due to pattern change) through a single repeater is less than $0.018 \mu\text{sec}$ (10° of clock shift). It is our purpose to show that these requirements have been met, and to investigate the various phenomena that may make the delay through a repeater pattern sensitive.

Fig. 58(a) shows the phase variation through eight repeaters excited by a long period of all pulses present, followed by a long period of one pulse out of eight present. It shows that the delay through a repeater varies about $0.009 \mu\text{sec}$ (5° of clock shift) as the pattern changes from the sparsest allowed to the densest possible. Measured pattern shift is shown in Fig. 58(b).

A simple model for phase accumulation (which treats the tank as a simple low-pass filter and neglects clock amplitude variation) along a string of repeaters predicts a maximum rate of change of clock phase, expressed in cycles per second, of $f_1 = \pi f_0 (\theta_0 / Q)$ where θ_0 is the shift per

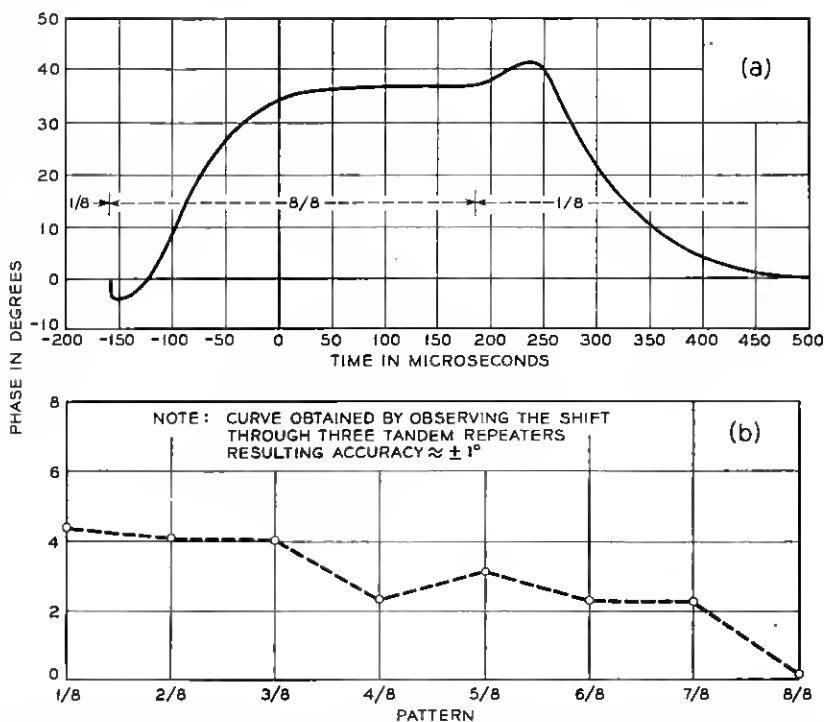


Fig. 58 — Measured clock pattern shift performance: (a) measured phase shift through eight repeaters due to abrupt change in pulse pattern; (b) measured phase shift per repeater due to change of pattern.

repeater in fraction of a time slot and Q is the quality factor of the repeater tank. From Fig. 58, f_1 is about 1.1×10^3 . The corresponding average effective $Q(\theta_0 = 5/360)$ is 60. Direct measurement indicates the actual circuit Q is the upper design value (≈ 100). There is reason to believe that the simple model, by neglecting the large clock amplitude variation with pattern, thus predicts a slower phase accumulation than actually is the case.

An attempt has been made to determine the contributors to the 5° of pattern shift per repeater. These measurements are very difficult, and the results are approximate only. There is indication that about half of the 5° comes from bottom-up clipping in the clock input stage, Q3 (see Fig. 31), and variations in the automatic clipping level with pattern. To separate the threshold and clock functions, C13 is used. An average voltage builds up across C13, dependent on the received pulse density, producing additional clipping via CR5 and CR6. This effect can be eliminated by use of a separate threshold amplifier, or by transformer coupling of the clock into Q3. The transformer primary would be made constant resistance by use of the appropriate RC network, so the operation of the clipping diode is not affected by the primary inductance of the transformer. Both solutions add slightly to the cost of the repeater.

It appears that the remaining two to three degrees is that expected due to clock extraction. The blocking oscillator does not seem to contribute significantly to pattern jitter. With the inductive load, the blocking oscillator compensates slightly for some of the shift introduced in clock extraction.

9.4 Temperature Performance

Expected range of temperature variation is 32 – 100°F for manhole-mounted repeaters and -40 to $+140^\circ\text{F}$ for units mounted above ground. The design range was -40 to $+140^\circ\text{F}$. The main effects of temperature are (1) effect on time crosshair position, and (2) effect on voltage crosshair position.

Fig. 59 shows the over-all effect of temperature on crosstalk performance for a repeater. This has been broken down into variation with clock position (by mistuning the tank) in Fig. 60 and variation with threshold in Fig. 61. It appears that the dominant effect is threshold variation with temperature, due primarily to the loss of dc gain in the threshold amplifier. The case shown is almost a worst case in that the threshold amplifier transistor was selected for approximately minimum

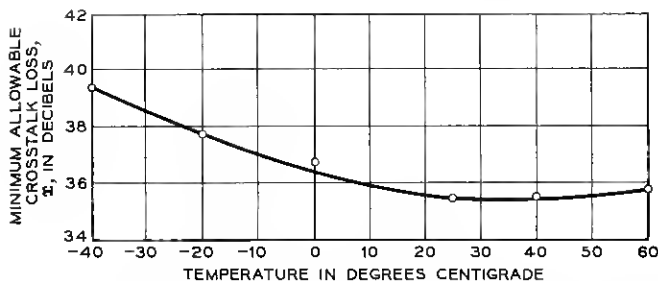


Fig. 59 — Typical measured over-all affect of temperature on crosstalk performance.

allowed β_0 . Some threshold temperature compensation is possible but has not been thoroughly investigated.

9.5 Field Experiment

Approximately 15 repeaters were installed on two two-way lines between Summit and South Orange, New Jersey. Twenty cable pairs were leased, and crosstalk and line loss measurements were made at all re-

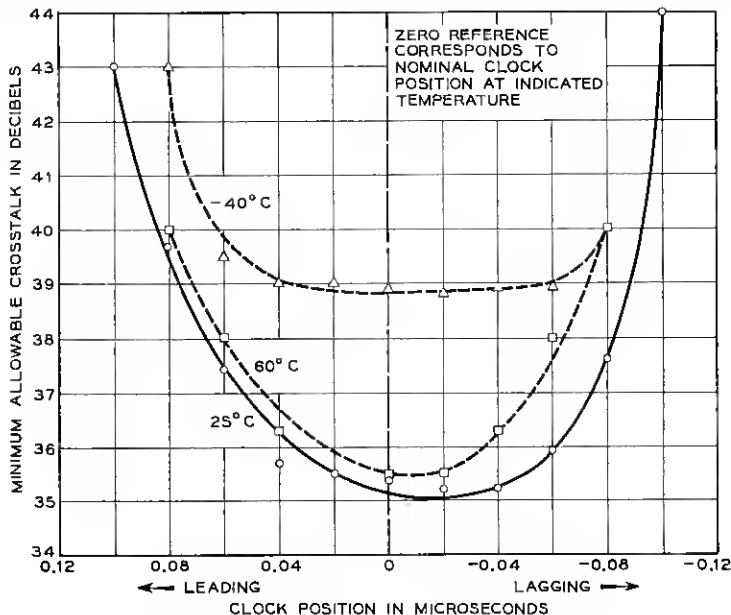


Fig. 60 — Typical crosstalk vs clock position.

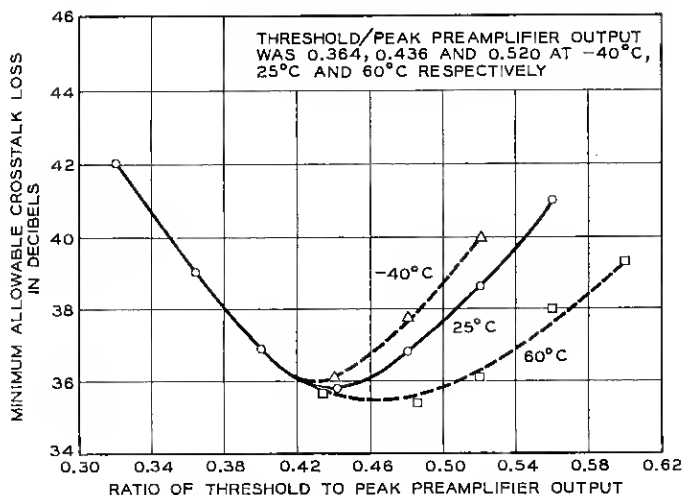


Fig. 61 — Typical crosstalk vs threshold.

peater points. One repeatered line was made up for maximum intra-system crosstalk (worse crosstalk pairs at each repeater point). The other line was of typical exposure. Placing the two lines in tandem gave one-way operation through 32 repeaters.

The resulting error rate was close to that which could be predicted from measured worst-case office impulse noise. Average error rates over a 10-minute interval were in the range 10^{-7} to 10^{-8} . About 50 per cent of the time the error rate over 10-minute intervals was less than 10^{-8} . In about 1 per cent of the 10-minute intervals the error rate exceeded 10^{-6} . These errors tended to come in short bursts and do not represent sustained error activity over the 10-minute interval.

X. CONCLUSIONS

A 1.544-mc experimental bipolar PCM repeater has been designed for one- or two-way use on unloaded exchange cable pairs. The circuit utilizes seven diffused-base transistors, and two repeaters with a common power unit are packaged in a can of $1\frac{1}{16} \times 3\frac{1}{8} \times 5\frac{3}{4}$ inches outside dimensions. The repeater includes power and line-length options, as well as provision for protection and remote testing, and is powered over the signal pair.

Timing jitter has been controlled to the extent required for 25-mile transmission, and the circuit has been optimized for near-end crosstalk performance.

Over sixty repeater circuits have been constructed, and measured performance is in reasonably good agreement with that predictable from design considerations.

Although many alternatives have been investigated for realization of each major function, one consistent design has been presented.

XI. ACKNOWLEDGMENT

The work reported herein has for the most part been carried out by various members of the Transmission Systems Development Department under the supervision of the author. At points the author has also drawn on the work of other departments. The guidance of E. E. Sumner and the prior work of F. T. Andrews are gratefully acknowledged.

REFERENCES AND BIBLIOGRAPHY

1. Aaron, M. R., this issue, p. 99.
2. Carbrey, R. L., Proc. I.R.E., **48**, p. 1546, Sept. 1960.
3. Davis, C. G., this issue, p. 1.
4. DeLange, O. E., B.S.T.J., **35**, p. 67, Jan., 1956.
5. DeLange, O. E., and Pustelnyk, M., B.S.T.J., **37**, p. 1487, Nov., 1958.
6. Mann, M., Straube, H. M., and Villars, C. P., this issue, p. 173.
7. Rowe, H. E., B.S.T.J., **37**, p. 1543, Nov. 1958.
8. Sunde, E. D., B.S.T.J., **36**, p. 891, July, 1957.
9. Thomson, W. E., Wireless Engineer, **29**, p. 256, Oct., 1952.
10. Wrathall, L. R., B.S.T.J., **35**, p. 1059, Sept. 1956.

